Zitteliana 97, 2023, 1–27 | DOI 10.3897/zitteliana.97.110677

SNSB Bayerische Staatssammlung für Paläontologie und Geologie

ZITTELIANA
An International Journal of Paleontology and Geobiology

Biostratigraphy and sedimentary sequences of the Toarcian Hainberg section (Northwestern Harz foreland, Northern Germany)

Gernot Arp[1], Yagmur Balmuk[1], Stephan Seppelt[2], Andreas Reimer[1]

1 *Georg-August-Universität Göttingen, Geowissenschaftliches Zentrum, Abteilung Geobiologie, Goldschmidtstraße 3, 37077 Göttingen, Germany*

2 *Platz 3, 31079 Sibbesse, Germany*

https://zoobank.org/A65FD6FB-F239-4EBA-8A3F-2054030CC9C9

Corresponding author: Gernot Arp (garp@gwdg.de)

Academic editor: Michael Krings ♦ **Received** 7 August 2023 ♦ **Accepted** 31 October 2023 ♦ **Published** 24 November 2023

Abstract

A temporary outcrop in southern Lower Saxony permitted the sedimentological, geochemical and palaeontological investigation of a 40.8 m thick Toarcian section, from the top of the Amaltheenton Formation, through the Posidonienschiefer and Jurensismergel Formations, to lower parts of the Opalinuston Formation. Bed by bed collected ammonites and belemnites, bivalve associations, as well as data from neighbouring sections indicate a largely complete sequence of ammonite zones and subzones for the Lower Toarcian. A prominent stratigraphic gap at the Posidonienschiefer/Jurensismergel Formation boundary probably comprises the Semipolitum Subzone as well as the Variabilis and Thouarsense Zones. Above a condensed Dispansum Zone follows the higher Upper Toarcian with a presumably largely complete sequence of zones and subzones, although direct evidence for this is only sporadic. However, a thin condensed bed with stromatolite crusts is recognisable at the boundary Pseudoradiosa to Mactra/Aalensis Subzone. The Toarcian/Aalenian boundary can only be drawn on basis of belemnite finds at another thin condensed bed. Only a few metres above, the Opalinum Zone is evident by ammonite findings.

Based on discontinuities, lithofacies, biofacies and correlations with neighbouring sections, a subdivision into alloformations, which largely correspond to formations, is applied. Based on that, a sequence stratigraphic interpretation with respect to third order transgression-regression cycles (T-R sequences) can be inferred: Above the regressive upper parts alloformation 1 (Amaltheenton Formation) with a maximum regression surface (mrs) near its top, the T-R sequence of the alloformation 2 (Posidonienschiefer Formation) is developed, with a maximum flooding surface (mfs) at the transition Falciferum/Commune Subzone and the regressive phase within the later Bifrons Zone. For the Commune Subzone, belemnite alignment indicates a seawater bottom current from SSE. The following maximum regression surface (mrs) lies near the Bifrons/Variabilis Zone boundary. The next sequence is not preserved at the studied location, but is preserved further East as well as further West, represented by the transgressive Dörnten Member (Variabilis and Thouarsense Zone). However, the regressive phase (Fallaciosum Subzone) is also missing there, indicated by a prominent sequence boundary with erosional relief at the base of the Dispansum Zone. The following alloformation 3 (Jurensismergel Formation and lowermost parts Opalinuston Formation) represents another T-R sequence with a maximum transgressive surface (base Mactra/Aalensis subzone) and a slightly thicker regressive Aalensis Subzone. The following maximum regression surface represents the boundary to alloformation 4 (major parts of Opalinuston Formation), followed again by a short transgressive phase (Pseudolotharingicum Subzone), condensation horizon and a longer regressive phase (Opalinum Zone).

These sequence stratigraphic interpretations are largely consistent with previous investigations in Northern and Southern Germany. Minor deviations in the timely position of maximum flooding and regression surfaces likely reflect effects of a higher subsidence at variable sedimentation rate in the North German Basin. With respect to the, at the site of investigation, incompletely exposed Opalinuston Formation, further studies on complete drill core sections are required.

Kurzfassung

Ein temporärer Aufschluss im südlichen Niedersachsen ermöglichte die sedimentologische, geochemische und paläontologische Untersuchung eines 40.8 m mächtigen Toarcium-Profils, vom Top der Amaltheenton-, über die Posidonienschiefer- und Jurensismergel-, bis zum tieferen Teil der Opalinuston-Formation. Horizontierte Ammoniten- und Belemnitenfunde, Bivalvenassoziationen, sowie Daten aus benachbarten Profilen lassen für das Untere Toarcium eine weitgehend vollständige Abfolge von Ammoniten-Zonen und -Subzonen erkennen. Eine markante Schichtlücke an der Posidonienschiefer/Jurensismergel-Formationsgrenze umfasst wahrscheinlich die Semipolitum-Subzone sowie die Variabilis- und Thouarsense-Zone. Über einer kondensierten Dispansum-Zone folgt das höhere Ober-Toarcium mit einer vermutlich weitgehend vollständigen, allerdings nur punktuell direkt belegbaren, Zonen- und Subzonen-Abfolge. Eine dünne, stromatolithführende Kondensationslage ist nur für den Grenzbereich Pseudoradiosa- zu Mactra/Aalensis-Subzone erkennbar. Die Grenze Toarcium/Aalenium kann nur mittels Belemnitenfunden an einer weiteren dünnen Kondensationlage festgelegt werden. Erst wenige Meter darüber kann die Opalinum-Zone mittels schlecht erhaltener Ammoniten wahrscheinlich gemacht werden.

Auf Grundlage von Diskontinuitäten, Lithofazies, Biofazies und Korrelationen mit Nachbarprofilen wird eine Unterteilung in Alloformationen, welche weitgehend den Formationen entsprechen, durchgeführt. Darauf aufbauend kann eine sequenzstratigraphische Interpretation bezüglich Transgressions-Regressions-Zyklen (T-R-Sequenzen) dritter Ordnung abgeleitet werden: Über dem regressiven höheren Teil der Alloformation 1 (Amaltheenton-Formation) mit einer maximalen Regressionsfläche (mrs) nahe seinem Top ist die T-R-Sequenz der Alloformation 2 (Posidonienschiefer Formation) entwickelt, mit einer maximalen Überflutungsfläche (mfs) am Übergang Falciferum/Commune-Subzone und nachfolgender regressiver Phase innerhalb der höheren Bifrons-Zone. Für die Commune-Subzone belegen eingeregelte Belemniten eine grundberührende Strömung aus südsüdwestlicher Richtung. Die nachfolgende maximale Regressionsfläche (mrs) liegt im Bereich der Bifrons/Variabilis-Zonengrenze. Die nächste Sequenz ist am untersuchten Profil nicht überliefert. Sie ist dagegen weiter östlich wie auch weiter westlich mit der transgressiven Dörnten-Subformation (Variabilis- und Thouarsense-Zone) erhalten geblieben. Die regressive Phase (Fallaciosum-Subzone) fehlt allerdings auch dort, angezeigt durch eine markante Sequenzgrenze mit Erosionsrelief an der Basis der Dispansum-Zone. Die Alloformation 3 (Jurensismergel- und tiefste Teile der Opalinuston-Formation) repräsentiert eine weitere T-R-Sequenz mit maximaler Überflutungsfläche (Basis Mactra/Aalensis-Subzone) und einer etwas längeren regressive Phase (Aalensis-Subzone). Die folgende maximale Regressionsfläche stellt die Grenze zur Alloformation 4 (Hauptteil der Opalinuston-Formation) dar, nachfolgend wieder mit kürzerer transgressiver Phase (Pseudolotharingicum-Subzone), Kondensationshorizont und längerer regressiver Phase (Opalinum-Zone).

Diese sequenzstratigraphischen Interpretationen stehen weitgehend in Einklang mit bisherigen Untersuchungen aus Nord- und Süddeutschland. Marginale zeitliche Abweichungen von maximalen Transgressions- oder Regressionsflächen spiegeln wahrscheinlich Effekte durch höhere Subsidenz bei variablen Sedimentationsraten im norddeutschen Becken wider. Für die am Untersuchungsort nur lückenhaft aufgeschlossene Opalinuston-Formation bedarf es weiterer Untersuchungen an vollständigen Kernprofilen.

Keywords

Ammonoidea, Jurensismergel Formation, Lower Jurassic, Northern Germany, Posidonienschiefer Formation, sealevel changes, stratigraphy

Schlüsselwörter

Ammonoidea, Jurensismergel-Formation, Meeresspiegel-Schwankungen, Norddeutschland, Posidonienschiefer-Formation, Stratigraphie, Unterer Jura

Introduction

The Lower Toarcian Posidonienschiefer Formation is considered as a fossil example of a climate change from cooler conditions with traces of glaciation to a greenhouse climate with increased temperatures, restricted ocean circulation, and oxygenation on shelf areas (i.e. the Toarcian Oceanic Anoxic Event T-OAE), with a consecutive extinction event (Jenkyns 1988; Palfy and Smith 2000; Dera and Donnadieu 2012; Ruebsam and Schwark 2021). For

a further understanding of the T-OAE, the documentation of many individual Posidonienschiefer Fm. sections and, based on that, the reconstruction of palaeogeography, sea level fluctuations and seawater current pattern are of fundamental importance. In turn, for the understanding of the recovery phase and stepwise vanishing of anoxic seafloor conditions after the T-OAE, the investigation of the subsequent Jurensismergel Formation is required.

Contrary to Southern Germany (e.g., Dotternhausen: Riegraf 1985; Röhl et al. 2001; Frimmel et al. 2004; Röhl and Schmid-Röhl 2005; Maisch 2021) the knowledge on biostratigraphy and sedimentary sequences of the Posidonienschiefer Formation in Northern Germany is still incomplete, despite the fact that the type locality of the formation (Hildesheim; Roemer 1836) is in this region (Fig. 1). However, much progress was achieved by the sequence stratigraphic investigations of drill cores in Northern Germany by Zimmermann et al. (2015).

Overview sections of the Toarcian of the investigation area (Fig. 1) have already been published in the classical works of Denckmann (1887, 1892), who demonstrated the principal lithological succession of the Posidonienschiefer Formation including the "Dörntener Schiefer", as well as the distinct erosive discontinuity at the contact to the following Jurensismergel Formation. Based on numerous exploration drillings, later researchers focussed on the organic geochemistry and source rock properties of the Posidonienschiefer Formation but also on palaeogeography and facies distribution (Dorn 1936; Brockamp 1944; Hoffmann 1968a; Schmitz 1968). Ammonite biostratigraphy of the lower and middle Posidonienschiefer Formation is discussed in Denckmann (1892), Hoffmann and Martin (1960), Hoffmann (1968a, b) and Weitschat (1973). Remarkable is the fragmentary documentation of the Toarcian section in the famous open pit mine Haverlahwiese, with scattered information in Hiltermann et al. (1960), Lehmann (1966), Schmitz (1968), Hoffmann (1968a), and Weitschat (1973). However, one of the few sedimentologically and palynologically well documented sections is that of Hildesheim-Itzum by Maul (1984), Riegel et al. (1986) and Loh et al. (1986), who also provided a palaeoenvironmental model for the Posidonienschiefer Formation of this region. Likewise well documented is the Posidonienschiefer Fm. of the Braunschweig area (e.g. Wunnenberg 1928, 1950; Brockamp 1944), especially due to a new drill core at Schandelah (van de Schootbrugge et al. 2019; Visetin et al. 2022).

With respect to the Upper Toarcian Jurensismergel Formation, early lithologic and biostratigraphic descriptions of sections are available in Ernst (1923–1924), Heidorn (1928) and Althoff (1936), summarized in Kumm et al. (1941). The commonly discontinuous sections with condensation and highly fluctuating thicknesses as well as the differently handled boundary to the Opalinuston Formation (partly resulting from a poor outcrop conditions) do not yet reveal any conclusive thickness and facies distribution patterns. Furthermore, section correlations are hampered by changing opinions on the identity of biostratigraphically important ammonites, especially with respect to the Toarcian-Aalenian boundary (e.g., *Pleydellia buckmani* Maubeuge and *Leioceras opalinum* (Reinecke)).

In 1975 and 1976, an exploration project of the Lower Saxony State Office for Soil Research (NLfB) on bituminous shales provided a number of drill cores, documented in unpublished short reports (Ringelheim 1–9, Hildesheim 1–4). Unfortunately these drillings have only been superficially investigated. Likewise, only short reports of iron ore exploration drillings of the Salzgitter AG 1938–1939 are available („Hainberg" 1 to 7, „Küchenhai" 1 and 2). In any case, the new sequence stratigraphic interpretation of the Lower Jurassic succession in Northern Germany mentioned above (Zimmermann et al. 2015), based on numerous drillings of hydrocarbon companies, forms a valuable basis for the present work.

Construction work at the motorway A7 between Bockenem and the Salzgitter junction exposed in September 2011 a section from the top parts of the Amaltheenton (Upper Pliensbachian), through the Posidonienschiefer and Jurensismergel (Toarcian) to the Opalinuston Formations (uppermost Toarcian to Lower Aalenian) at the foothill of the Hainberg (Fig. 1).

The aim of the study is to document the sedimentary succession and biostratigraphy of this almost continuous section of the Toarcian at a classical location (i.e., Hainberg; Denckmann 1892) in Northern Germany and to discuss its implications for sealevel changes and palaeogeography.

Location and geological overview

The investigated section "Hainberg" is a motorway cutting located in Northern Germany, Lower Saxony, approximately 18 km ESE of Hildesheim (Fig. 1) at the motorway A7 (Hannover-Kassel) immediately south of the resting place "Sillium-Ost". The coordinates of the section, located on the topographic map 1:25000, sheet 3927 Ringelheim are 52°3.250781'N, 10°11.397949'E to 52°3.465281'N, 10°11.517376'E, at an elevation of ca. 150–155 m a.s.l. at the western foot of the "Hainberg". The exposure of the motorway cutting was about 350 m long, with up to 4 m height.

The Hainberg is situated in the northern foreland of the Harz Mountains at the southern margin of the North German Basin. The area is composed of gentle synclines and anticlines of Mesozoic sedimentary rocks, overlying Permian evaporites (Zechstein Group) and the Variscan basement of the deep subsurface (Fig. 1). The latter, at 2.0–2.3 km depth, is composed of folded Palaeozoic greywackes and shales, which are exposed further SE in the Harz Mountains. The Permian comprises minor continental siliciclastics (70–140 m Rotliegend Group) and a thick sequence of marine evaporites (600–1200 m Zechstein Group), which commonly form salt diapirs. The Mesozoic cover sequence starts with continental siliciclastics of

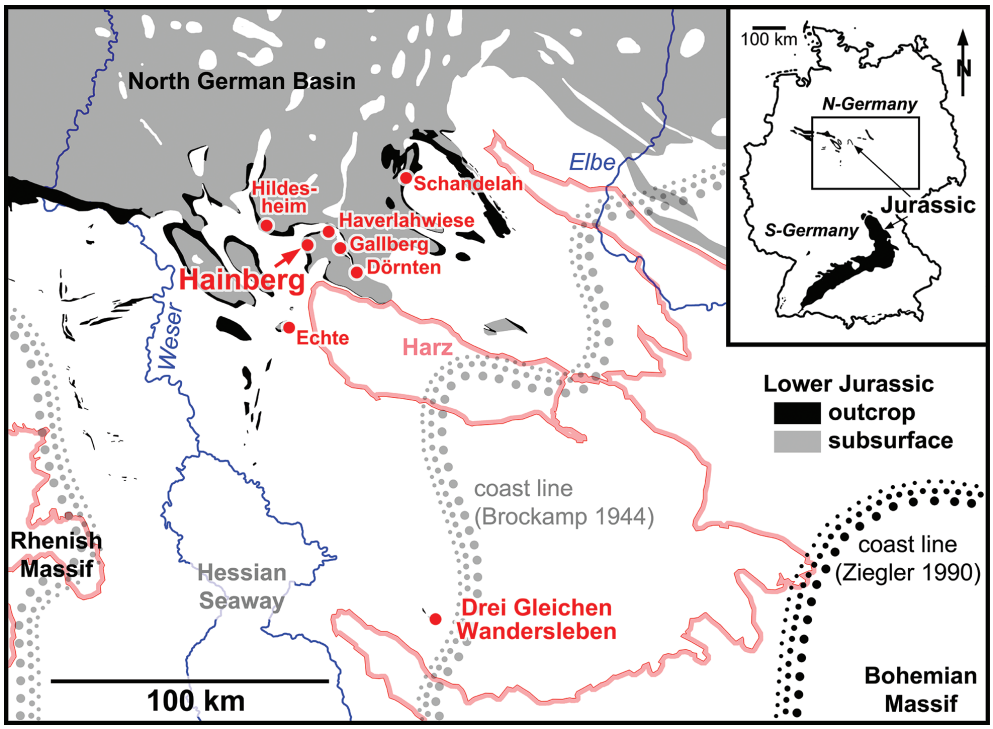

Figure 1. Geographic and geological overview with the location of the Hainberg section and further locations of Toarcian sections in Northern Germany. Outcrop and subsurface deposits of Lower Jurassic after Arnold et al. (1973), Duphorn et al. (1974), Motzka et al. (1979), Waldeck (1986), Kriebel et al. (1998), Motzka-Nöring (1998), Seidel et al. (1998), Radzinski et al. (1999), Knoth et al. (2000), Martiklos (2002), and Reinhold et al. (2008). Supposed former coastlines of the Toarcian after Brockamp (1944; outdated) and Ziegler (1990). Areas outlined in red are Variscan basement rocks, uplifted during the Cretaceous.

the Lower Triassic Buntsandstein Group (700–950 m), followed by marine carbonates of the Middle Triassic Muschelkalk Group (275–290 m) and again continental red beds of the Upper Triassic Keuper Group (ca. 350 m) (Schröder 1912; Dahlgrün 1939; Look et al. 1984, 1986; Jordan 1989).

At the western slope of the Hainberg, which is part of the Ringelheim Syncline, Lower Jurassic strata of the Schwarzjura Group (Franz et al. 2020) show a 300–350 m thick succession of dark calcareous claystones, with the 27–30 m thick Posidonienschiefer Fm. and a less than 1 m thick Jurensismergel Fm. at its top. Of the following Braunjura Group, up to 300 m dark marine claystones are preserved, cut at their top by an angular unconformity. Younger Jurassic strata as well as major parts of the Lower Cretaceous strata are absent. Albian to Santonian strata of the Hilssandstein Fm., Alfeld Fm., Plänerkalk Group, and Emscher Fm. (Hiss et al. 2005), together up to 520 m thick, follow from the top of the Hainberg to the centre of the Ringelheim Syncline, which is covered by Quaternary sediments (Look et al. 1984, 1986).

The folding of the Mesozoic strata into synclines and anticlines is due to a combination of tectonic faults in the Variscan basement and halotectonic movements of the Zechstein Group (Martini 1953; Jordan 1989). These combined ortho- and halotectonic movements were active during the Triassic, Late Jurassic and, with increasing intensity, during the Santonian to Campanian, when the Harz Mountains were uplifted (Voigt et al. 2004; von Eynatten et al. 2008). For the Early Jurassic, such tectonic movements in Northern Germany have been inferred from increased strata thickness at the margin of salt diapirs (e.g. drilling Etzel 24; Hoffmann 1968a; drilling Hamburg Allermöhe 1; Zimmermann et al. 2015) and thin, iron-oolitic deposits at salt pillows (e.g., Fallstein; Thomas 1924; Ott 1967). Indeed, the Hainberg section lies at the western margin of the Eichsfeld-Altmark High, a Permotriassic tectonic high (Paul 1993), which was active at least to Late Triassic times (Barnasch et al. 2005).

At the site of investigation, the strata were 10° inclined towards ENE (70°). Further uplift of the whole region, from a near sealevel position to the present day elevation took place after the Oligocene (e.g. Jordan et al. 1994: p. 68). The present-day geomorphology is essentially the result of an intense Miocene-Pliocene weathering, followed by Pleistocene erosion with frost wedging and solifluction (e.g. Brosche 1996), which also shaped the ridge of the Hainberg and covered its lower slopes with debris (Look et al. 1984, 1986; Heunisch et al. 2017).

Materials and methods

Fieldwork and sampling was carried out on three days in September 2011. Lithological descriptions are based on field observation and binocular observations on hand specimens, supplemented by eight thin sections of 28×48 mm and 7.5×10 cm in size, and about 50 µm thickness.

Total carbon (C_{tot}), total nitrogen (N_{tot}), and total sulphur (S_{tot}) of 50 bulk rock samples (Table 1) were analysed with a Euro EA 3000 Elemental Analyser (HEKAtech, Wegberg, Germany) applying 2,5-bis(5-tertbenzoxazol-2-yl) thiophene (BBOT) and atropine sulphate monohydrate (IVA Analysentechnik, Meerbusch, Germany) as reference material. Organic and carbonate carbon (C_{org}, C_{carb}) contents were determined by a LECO RC612 (Leco, St. Joseph, MI, USA) multi-phase carbon and water analyser. For calibration, Leco synthetic carbon (1 and 4.98 carbon %) and Leco calcium carbonate (12 carbon %) standards were used. All analyses were performed as duplicates. Analytical accuracy of all analyses was better than 3%. The carbonate-free fraction was calculated from the total weight minus the $CaCO_3$ and C_{org} content. Biostratigraphy is based on 24 determinable ammonites that were recovered *in situ*. Ammonite determinations were made using the descriptions of the type specimens and the systematic descriptions in Howarth (1992), Schulbert (2001), Rulleau (2007), Lacroix and Le Pichon (2011), Rulleau et al. (2013), and Di Cencio and Weis (2020). Belemnite determinations were made using Kolb (1942), Schlegelmilch (1998), Weis (1999), Riegraf (2000) and Arp (2010).

Orientation of belemnite rostra of two beds (n = 79 and 104) was measured in the field using a Freiberg Geological Compass. Graphical analysis was carried out using the program StereoNett Version 2.46 (Duyster 2000).

Repository: The material is stored in the Museum and Collection of the Geoscience Centre, University of Göttingen, under the numbers GZG.INV.866–GZG.INV.920.

Data Availability Statement: All data used in this publication, supplementary figures and tables are stored on the Göttingen Research Online Data repository (https://doi.org/10.25625/UEELUH).

Figure captions: unless otherwise noted, all specimen are coated by ammonium chloride prior to photography. Abbreviations: diameter (d), diameter of penultimate half whorl (d_i), umbilical width (u), whorl height (wh), whorl breadth (wb), primary ribs per half whorl (rb/2) (Howarth 1992). Shell parameters are given in brackets, when precise measurements were not possible due to poor preservation.

Results

Description of the section

Informal bed names are given in quotation marks. An overview of the section is provided in Fig. 2. Ammonites and belemnite findings are illustrated in Figs 3–26. The strata are described from bottom to top:

Amaltheenton Formation:

Bed 1: >100 cm medium-grey, well bedded claystone with white-grey quartz silt and fine-grained mica layers;
Bed 2: 1 cm rust-brown layer of siderite nodules;
Bed 3: 230 cm medium-grey, well bedded claystone with white-grey quartz silt and fine-grained mica layers (with small-scale cross stratification);
Bed 4: 2 cm rust-brown layer of siderite nodules;
Bed 5: 60 cm medium-grey, well bedded claystone with white-grey quartz silt and fine-grained mica layers;
Bed 6: 8 cm light-grey to white-grey, well bedded silty claystone with fine-grained mica.

Posidonienschiefer Formation:

Bed 7: 15 cm rust-brown/yellowish-brown varved, laminated clay with fine-grained mica and black manganese coatings on bedding planes and fractures;
Bed 8: 5 cm light-grey/middle-grey varved, laminated clay with yellow-brown weathered layers of former iron sulphides, abundant fine-grained mica on bedding planes;
Bed 9: 40 cm grey to yellow-brown weathered, laminated bendable clay with few fish scales and teeth; ammonoids: *Dactylioceras* cf. *crosbeyi* (Simpson) (compressed; Fig. 3);
Bed 10: 40 cm dark-grey bituminous calcareous claystone with even lamination and minor fish scale debris; ca. 10 above basis one 8 cm thick lenticular limestone concretion ("Elegantulum Concretion"); ammonoids: *Eleganticeras elegantulum* (Young & Bird) (in concretion; Fig. 27), 10 cm above basis *Eleganticeras* sp. (compressed); other fossils: *Lepidotes elvensis* (de Blainville) (Fig. 27), *Meleagrinella* (*Clathrolima*) sp.; *Coelodiscus minutus* (Schübler in Zieten);
Bed 11: 0–18 cm "Boreale Concretions": medium grey laminated bituminous limestone concretions (pellet packstone) up to 50 cm width, with scattered mm-sized holoplanktonic gastropods in layers, fine-grained shell debris and minor fish scale debris; ammonoids: *Hildaites murleyi* (Moxon) (Fig. 4); other fossils: *Coelodiscus minutus* (Schübler in Zieten), abundant *Parainoceramya dubia* (Sowerby);
Bed 12: 150 cm dark-grey laminated bituminous marl to calcareous marl; minor fine-grained shell and fish scale debris; ammonoids: *Lytoceras* sp. (compressed; 75 cm above basis; Fig. 5); other fossils: *Meleagrinella* (*Clathrolima*) sp. (layers with poorly preserved specimens 10–15 and 140 cm above basis; *Parainoceramya dubia* (Sowerby) (75 cm above basis; Fig. 5);
Bed 13: 15 cm dark-grey laminated bituminous argillaceous limestone with fine-grained shell debris and minor fish scale debris; ammonoids: *Lytoceras* sp. (compressed), *Eleganticeras* sp. (compressed), other fossils: several bedding planes with abundant *Bositra buchi* (Roemer) up to 8 mm in size, few small *Parainoceramya dubia* (Sowerby), *Meleagrinella* (*Clathrolima*) sp.;
Bed 14: 25 cm dark-grey laminated bituminous calcareous marl with fine-grained shell debris and minor fish scale debris; fossils: *Meleagrinella* (*Clathrolima*) sp.;

Table 1. Carbon, sulphur, and nitrogen contents of sedimentary rocks of the Hainberg section.

Sample Number	Formation	Bed Number	Section meter	Lithology	Remarks	C_{tot} mean	C_{org} mean	C_{carb} mean	$CaCO_3$ calculated	C_{org} carbonate-free	N_{tot} mean	S_{tot} mean	S_{tot} carbonate-free
			[m] from top			[wt %]	[wt %]	[wt %]	[wt %]	[wt %]	[wt %]	[wt %]	[wt %]
sil1	Opalinuston	41	-0.25	weathered clay	affected by solifluction	1.98	1.95	0.03	0.25	1.95	0.10	0.75	0.75
sil2	Opalinuston	40	-1.7	claystone		1.20	0.97	0.23	1.92	0.99	0.07	0.05	0.05
sil3	Opalinuston	38	-2.65	claystone		0.67	0.56	0.11	0.92	0.57	0.06	0.05	0.05
sil4	Opalinuston	36	-2.77	calcareous claystone	matrix between concretions	3.25	0.51	2.74	22.8	0.66	0.05	0.04	0.05
sil5	Opalinuston	35	-3.1	claystone		1.03	0.66	0.37	3.08	0.68	0.06	1.40	1.45
sil6	Opalinuston	34	-13.35	claystone		1.16	0.59	0.57	4.75	0.62	0.06	0.04	0.04
sil7	Opalinuston	32	-13.7	marlstone	matrix between concretions and stromatolites	5.68	0.41	5.27	43.9	0.73	0.04	0.01	0.02
sil8	Opalinuston	31	-14.0	claystone		1.09	0.99	0.10	0.83	1.00	0.07	0.04	0.04
sil9	Opalinuston	31	-14.85	claystone		1.38	1.06	0.32	2.67	1.09	0.07	0.04	0.04
sil10	Opalinuston	31	-15.7	claystone		1.23	1.09	0.14	1.17	1.10	0.07	0.17	0.17
sil11	Jurensismergel	29	-16.2	calcareous marlstone	echinoderm packstone	8.24	0.36	7.88	65.7	1.05	0.03	0.08	0.23
sil12	Jurensismergel	28	-16.3	calcareous claystone	matrix of „zeta conglomerate“	2.36	0.97	1.39	11.6	1.10	0.07	0.03	0.03
sil13	Jurensismergel	27	-16.4	calcareous claystone	middle part of „oolite marl“	2.39	1.08	1.31	10.9	1.21	0.07	0.04	0.04
sil14	Jurensismergel	27	-16.5	calcareous claystone	lower part „oolite marl“	2.77	1.07	1.70	14.2	1.25	0.07	0.07	0.08
sil15	Jurensismergel	27	-16.55	marlstone	basis „oolite marl“, matrix between belemnites	5.97	1.71	4.26	35.5	2.65	0.07	1.49	2.31
sil16	Posidonienschiefer	26	-16.6	calcareous marlstone	„fucoid bed equivalent“	10.9	2.43	8.44	70.3	8.19	0.07	0.05	0.17
sil17	Posidonienschiefer	25	-16.9	claystone	bituminous	12.1	12.0	0.07	0.58	12.1	0.34	3.78	3.81
sil18	Posidonienschiefer	24	-19.2	calcareous claystone	bituminous	12.6	9.96	2.67	22.2	12.8	0.27	0.95	1.22
sil19	Posidonienschiefer	24	-21.7	calcareous claystone	bituminous	14.3	11.8	2.47	20.6	14.9	0.34	2.72	3.42
sil20	Posidonienschiefer	24	-25.2	argillaceous marlstone	bituminous	12.5	8.38	4.14	34.5	12.8	0.24	2.04	3.11
sil21	Posidonienschiefer	24	-26.2	argillaceous marlstone	bituminous	12.8	9.19	3.61	30.1	13.1	0.26	1.29	1.84
sil22	Posidonienschiefer	24	-29.3	argillaceous marlstone	bituminous	12.5	8.77	3.68	30.7	12.6	0.26	1.26	1.81
sil23	Posidonienschiefer	24	-32.2	calcareous claystone	bituminous	14.1	11.3	2.78	23.2	14.7	0.31	1.96	2.55
sil24	Posidonienschiefer	24	-33.2	calcareous claystone	bituminous	16.1	13.4	2.71	22.6	17.3	0.36	2.70	3.49
sil25	Posidonienschiefer	24	-34.3	calcareous claystone	bituminous	14.4	11.6	2.72	22.7	15.0	0.31	0.73	0.95
sil26	Posidonienschiefer	24	-35.1	calcareous claystone	bituminous	13.8	11.2	2.56	21.3	14.2	0.28	0.78	0.99
sil27	Posidonienschiefer	23	-35.23	argillaceous marlstone	bituminous martix of belemnite accumulation	12.4	8.97	3.38	28.2	12.5	0.24	0.58	0.81
sil28	Posidonienschiefer	22	-35.25	argillaceous limestone	„Monotis event bed“	11.7	0.74	11.0	91.5	8.70	0.02	0.02	0.24
sil29	Posidonienschiefer	21	-35.3	marlstone	bituminous	13.8	7.07	6.73	56.1	16.1	0.22	1.07	2.42
sil30	Posidonienschiefer	21	-35.45	marlstone	bituminous	14.7	8.11	6.54	54.5	17.8	0.23	1.01	2.23
sil31	Posidonienschiefer	21	-35.6	argillaceous marlstone	bituminous	17.0	13.5	3.48	29.0	19.0	0.35	1.08	1.52
sil32	Posidonienschiefer	20	-35.7	argillaceous limestone	bituminous	14.1	5.16	8.96	74.7	20.4	0.13	1.56	6.15
sil33	Posidonienschiefer	19	-35.8	calcareous marlstone	bituminous	14.3	6.23	8.09	67.4	19.1	0.17	0.28	0.87
sil34	Posidonienschiefer	18	-36.0	argillaceous limestone	bituminous	13.9	4.40	9.48	79.0	21.0	0.11	0.51	2.42
sil35	Posidonienschiefer	17	-36.65	marlstone	bituminous	17.4	11.2	6.25	52.1	23.4	0.30	1.81	3.77
sil36	Posidonienschiefer	17	-37.25	marlstone	bituminous	18.6	13.3	5.28	44.0	23.7	0.34	1.64	2.93
sil37	Posidonienschiefer	17	-39.0	marlstone	bituminous	17.8	12.8	4.98	41.5	21.9	0.32	0.68	1.15
sil38	Posidonienschiefer	16	-39.65	argillaceous marlstone	bituminous	21.1	18.0	3.06	25.5	24.2	0.44	1.23	1.65
sil39	Posidonienschiefer	15	-40.0	argillaceous limestone	„Elegans Bed“, bituminous	12.9	3.17	9.73	81.1	16.8	0.08	0.27	1.44
sil40	Posidonienschiefer	14	-40.35	calcareous marlstone	bituminous	13.8	5.65	8.10	67.5	17.4	0.14	0.21	0.66
sil41	Posidonienschiefer	13	-40.55	argillaceous limestone	bituminous	13.5	4.35	9.12	76.0	18.1	0.11	1.14	4.73
sil42	Posidonienschiefer	12	-40.75	marlstone	bituminous	14.5	7.45	7.09	59.1	18.2	0.19	0.53	1.29
sil43	Posidonienschiefer	12	-41.15	calcareous marlstone	bituminous	14.8	6.96	7.82	65.2	20.0	0.16	0.29	0.84
sil44	Posidonienschiefer	12	-41.65	argillaceous marlstone	bituminous	15.1	12.0	3.08	25.7	16.2	0.32	0.55	0.75
sil45	Posidonienschiefer	12	-42.0	argillaceous marlstone	bituminous	17.0	13.1	3.96	33.0	19.5	0.37	0.57	0.85
sil46	Posidonienschiefer	11	-42.25	argillaceous limestone	„Boreale Nodule“, bituminous	12.7	1.33	11.3	94.3	23.5	0.04	0.20	3.58
sil47	Posidonienschiefer	10	-42.5	calcareous claystone	bituminous	23.4	22.1	1.23	10.2	24.7	0.56	1.67	1.86
sil48	Posidonienschiefer	9	-42.95	claystone		0.84	0.81	0.03	0.25	0.81	0.09	0.05	0.05
sil49	Posidonienschiefer	8	-43.15	claystone	with fine-grained mica	0.54	0.52	0.02	0.17	0.52	0.07	0.03	0.03

Sample Number	Formation	Bed Number	Section meter	Lithology	Remarks	C_{tot} mean	C_{org} mean	C_{carb} mean	$CaCO_3$ calculated	C_{org} carbonate-free	N_{tot} mean	S_{tot} mean	S_{tot} carbonate-free
			[m] from top			[wt %]	[wt %]	[wt %]	[wt %]	[wt %]	[wt %]	[wt %]	[wt %]
sil50	Posidonienschiefer	7	-43.25	claystone	rust-brown basal layer	0.84	0.82	0.02	0.17	0.82	0.07	0.07	0.07
sil51	Amaltheenton	6	-43.4	claystone	with quartz silt and fine-grained mica	0.30	0.28	0.02	0.17	0.28	0.05	0.31	0.31
sil52	Amaltheenton	3	-44.3	claystone	with quartz silt and fine-grained mica	0.34	0.32	0.02	0.17	0.32	0.05	0.13	0.13
sil53	Amaltheenton	3	-45.6	claystone	with quartz silt and fine-grained mica	0.56	0.54	0.02	0.17	0.54	0.05	0.31	0.31
sil54	Amaltheenton	1	-46.8	claystone	with quartz silt and fine-grained mica	0.72	0.69	0.03	0.25	0.69	0.07	0.31	0.31

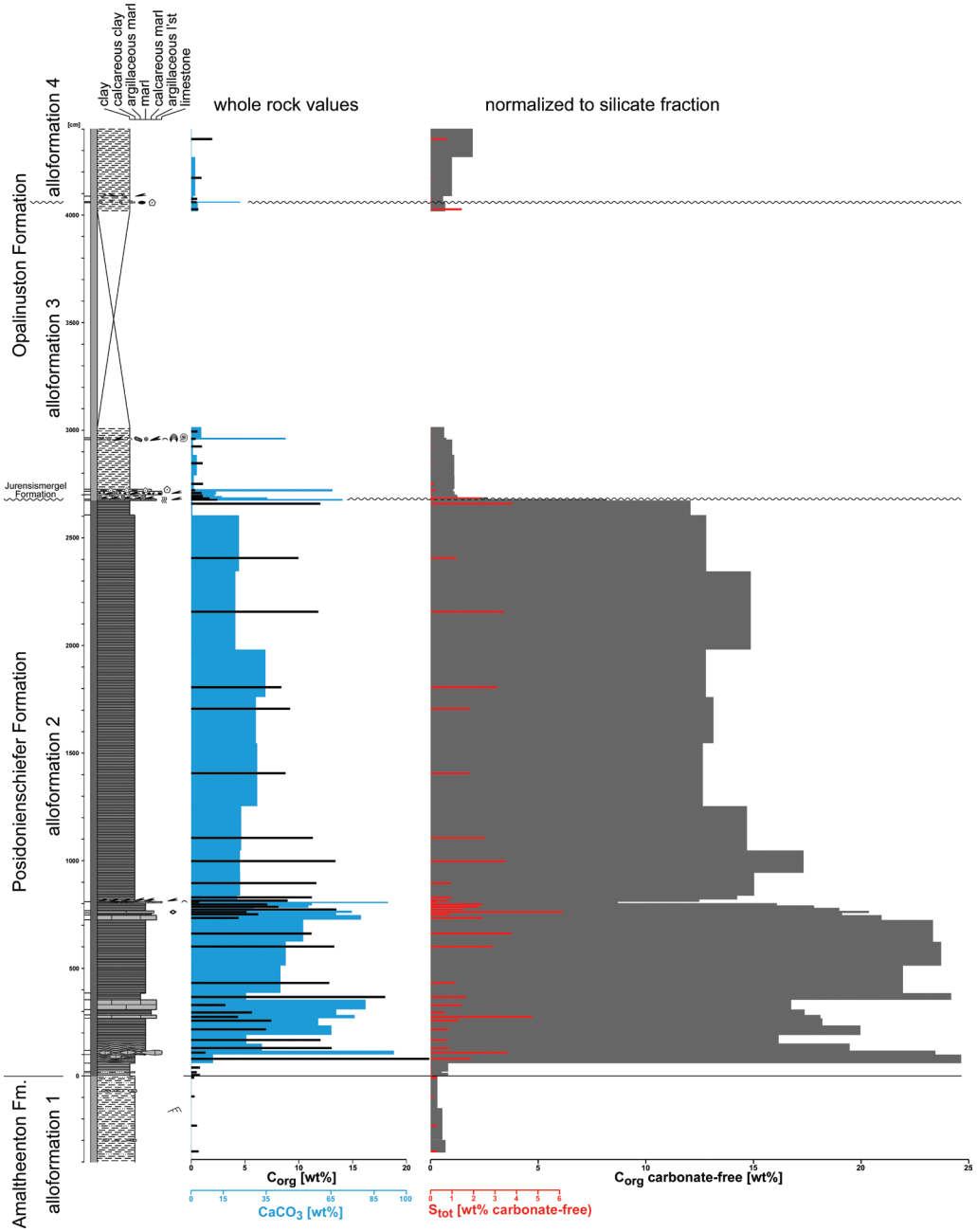

Figure 2. Overview on lithology and lithostratigraphy of the Hainberg section (top Amaltheenton Fm. to lower Opalinuston Fm.) with $CaCO_3$, organic carbon, and sulphur contents. For legend see Fig. 28.

Bed 15: 45 cm "Lower Elegans Bed": dark-grey laminated bituminous argillaceous limestone with fine-grained shell debris and rare fish scales; ammonoids: *Eleganticeras elegans* (Sowerby) (compressed; Fig. 6); other fossils: two aptychae, one fragmentary fish remain (*Tetragonolepis*?);

Bed 16: 30 cm dark-grey to black, highly bituminous laminated argillaceous marl with fine-grained shell debris; fossils: several bedding planes with pavements of *Bositra buchi* (Roemer) (up to 8 mm in size); one *Parainoceramya dubia* (Sowerby);

Bed 17: 340 cm dark-grey to black, bituminous laminated marl with fine-grained shell debris and rare fish scales; minor fine-grained carbonaceous plant debris; ammonoids: *Harpoceras* sp. (compressed fragment 50 cm above basis); other fossils: *Parainoceramya dubia* (Sowerby) (common 220 and 280 cm above basis);

Bed 18: 22 cm dark-grey, bituminous laminated calcareous limestone full of *Bositra* shell debris and abundant fish scales in layers; fossils: *Bositra buchi* (Roemer);

Bed 19: 10 cm dark-grey, bituminous laminated calcareous marl full of *Bositra* valves and shell debris; uneven bedding planes; fossils: *Bositra buchi* (Roemer);

Bed 20: 10 cm dark-grey, bituminous laminated calcareous marl to argillaceous limestone; fish scale debris in layers;

Bed 21: 40 cm dark-grey, bituminous laminated marl full of *Bositra buchi* valves up to 12 mm in size; uneven bedding planes;

Bed 22: 1 cm "Monotis Bed": medium-grey, microcrystalline argillaceous limestone composed of numerous *Meleagrinella* (*Clathrolima*) *substriata* (Münster) (see Lutikov and Arp 2022 for taxonomy);

Bed 23: 2 cm "Commune belemnite battlefield": dark-grey, rust-brown oxidized, bituminous laminated argillaceous marl with numerous, current-aligned belemnite rostra; belemnites poorly preserved due to pyrite oxidation; ammonoids: *Dactylioceras* sp. (compressed; Fig. 7); other fossils: *Acrocoelites* sp. (Fig. 8), *Dactyloteuthis irregularis* (Fig. 9), *Stenopterygius* sp. (rib fragments);

Bed 24: ca. 18 m dark-grey bituminous laminated calcareous claystone to argillaceous marl; scattered compressed marcasite nodules; even bedding planes; lower 10 m with bedding planes full of *Bositra* shell debris and few complete *Bositra buchi* valves (up to 5 mm in size); uppermost 8 m with decreasing fine-grained *Bositra* shell debris, increasing carbonaceous plant debris and mica flakes; partially fossil-free-layers; compressed ammonoids *Dactylioceras* cf. *commune* (Sowerby) (5 cm above basis); other fossils: *Bositra buchi* (Roemer), ostracods (uppermost 2 m), one mm-sized pellet composed of fish remains (2 m below top);

Bed 25: 60 cm medium-grey to brownish, bituminous laminated claystone; with minor fine-grained shell debris at its top;

Bed 26: 0–6 cm "fucoid bed equivalent": medium-grey, laminated lenticular to irregularly shaped calcareous marl to argillaceous limestone concretions with calcite or marcasite-filled burrows (0.5 cm diameter); thin layers with white, fine-grained shell debris; sharp upper boundary, with impressions of ooids from the bed above.

Jurensismergel Formation:

Bed 27: 20 cm "Oolite marl with belemnite accumulation": indistinctly bedded, medium-grey marl with numerous bioclasts, iron ooids and cm-sized white, ooid-bearing phosphorite nodules; iron ooids 1–2 mm in size and colonized by nubeculariid foraminifera; belemnite accumulation at the basis of the bed; ammonoids: *Osperleioceras* cf. *beauliziense* (Monestier) (5 cm above basis) (Fig. 10); *Perilytoceras* sp.; other fossils: *Dactyloteuthis irregularis* (Schlotheim) (mass accumulation), *Chlamys textoria* (Schlotheim), *Liostrea erina* (d'Orbigny), *Parainoceramya* sp., *Chladocrinus* sp., ostracods, *Chondrites* sp.;

Bed 28: 15 cm "Zeta Conglomerate": indistinctly bedded, medium-grey marl with iron ooids, bioclasts and numerous reworked rust-brown, cm-sized concretions (intraclast rudstone); abundant phosphoritic ammonite casts and reworked fragments; abundant nubeculariid foraminifera on ooids, echinoderm debris and other bioclasts; belemnite accumulation at the basis of the bed; ammonoids: *Phlyseogrammoceras dispansiforme* (Wunstorf) (Figs 11, 12), *Phlyseogrammoceras transiens* (Ernst) (Fig. 13), ?*Alocolytoceras* sp. (Fig. 14); *Dumortieria* sp. (juvenile, fragment from top of the bed); other fossils: *Dactyloteuthis similis* (Seebach) (mass accumulation), *Palaeonucula hammeri* (Defrance), *Sphenodus* sp.; bryozoan colonies on shell fragments;

Bed 29: 10 cm medium-grey, massive calcareous marl full of echinoderm remains (echinoderm packstone with micritic matrix) with abundant iron as well as calcareous ooids, abundant nubeculariid foraminifera at the surface of ooids, echinoderm ossicles and rounded shell fragments, echinid spines, bivalve shell; indistinct lower boundary;

Bed 30: 2 cm fibrous calcite with cone-in-cone structures.

Opalinuston Formation:

Bed 31: 230 cm medium-grey, well-bedded claystone; few layers with fine-grained white shell debris of *Bositra* 25–40 cm and 120–140 cm above basis; thin marcasitic burrows; ammonoids: indeterminable compressed ammonite with bundled sinuous ribs; other fossils: *Bositra suessi* (Oppel) (25 cm above basis);

Bed 32: 6–8 cm dark-grey, well bedded marl full of fine-grained shell debris, abundant limonitic iron ooids, belemnite rostra and cm-sized white-grey, corroded phosphorite nodules; near the basis rust-brown irregular argillaceous limestone concretions and large compressed ammonite shell fragments (> 15 cm) with mm-thin stromatolitic crusts;

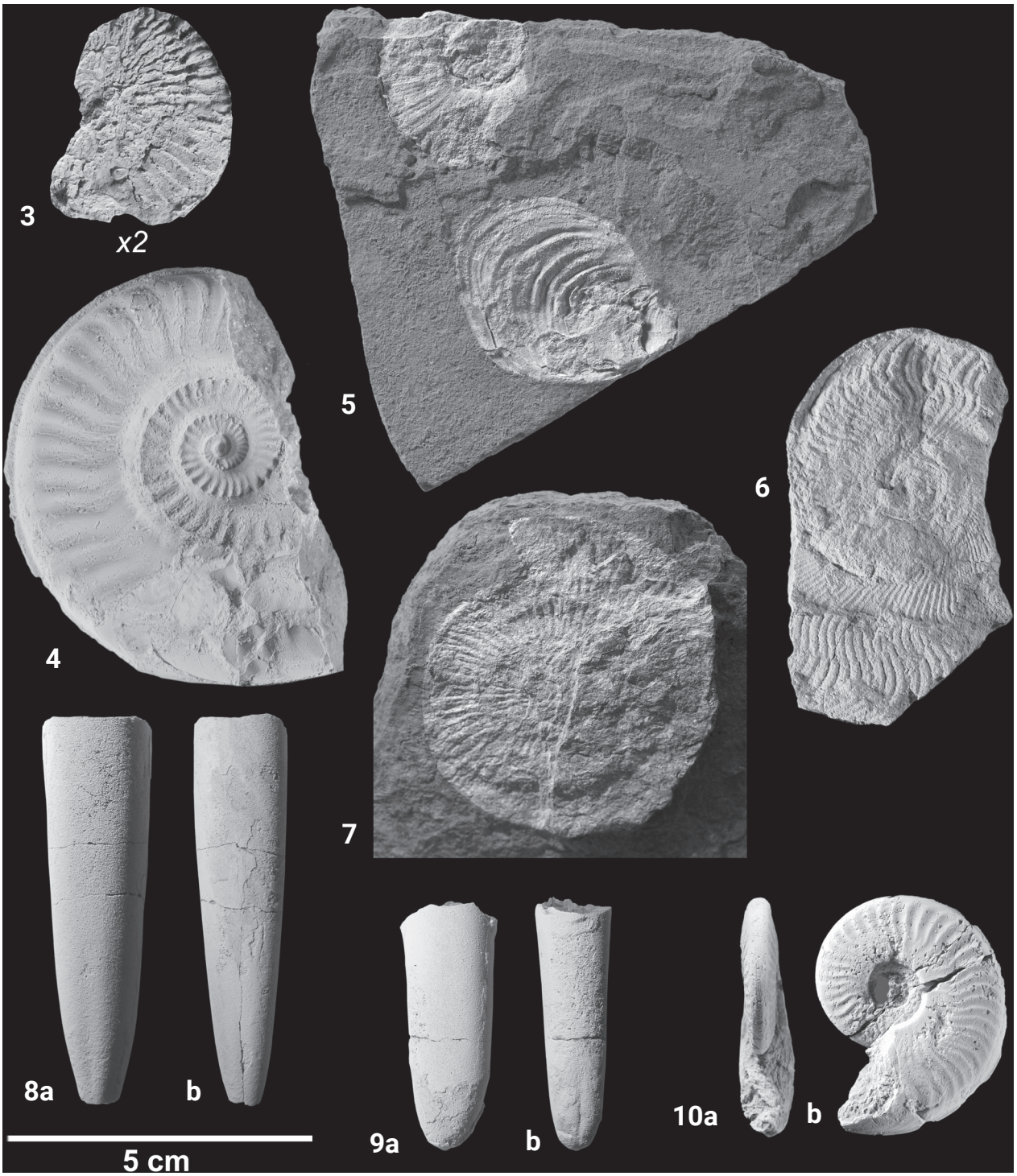

Figures 3–10. Ammonites and Belemnites of the Toarcian Hainberg section **3**. *Dactylioceras* cf. *crosbeyi* (Simpson), bed 9, Posidonienschieder Formation, Tenuicostatum Zone. GZG.INV.866: d = (21) mm, n = (7), wh = (8) mm, rb/2 = (20); **4**. *Hildaites murleyi* (Moxon), bed 11 "Boreale Concretions", Posidonienschiefer Formation, Exaratum Subzone. GZG.INV.867: d = 75 mm, di = 53 mm, u = 30 mm, wh = 23 mm, wb = (17) mm, rb/2 = (20); **5.** *Lytoceras* sp. und *Parainoceramya dubia* (Sowerby), bed 12, Posidonienschiefer Formation, Exaratum/Elegans Subzone. GZG.INV.868: d = (33) mm, u = (10) mm, wh = 14 mm; **6.** *Eleganticeras elegans* (Sowerby), bed 15, Posidonienschiefer Formation, Elegans Subzone. GZG.INV.869: d = 66 mm, di = (42) mm, u = (13) mm, wh = (36) mm; **7.** *Dactylioceras* (*Dactylioceras*) cf. *commune* (Sowerby), 5 cm above basis of bed 24, Posidonienschiefer Formation, Commune Subzone. GZG.INV.870: d = 53 mm, di = (42) mm, u = (27) mm, wh = (12) mm; **8.** *Acrocoelites* sp., left: lateral view, right: ventral view, bed 23, Posidonienschiefer Formation, Commune Subzone. GZG.INV.871: Length = 63.5 mm (incomplete: without alveolar region); **9.** *Dactyloteuthis irregularis* (Schlotheim) [syn.: *Dactyloteuthis digitalis* (Blainville)], left: lateral view, right: ventral view, bed 23, Posidonienschiefer Formation, Commune Subzone. GZG.INV.872: Length = 40.5 mm; **10.** *Osperleioceras* cf. *beauliziense* (Monestier), bed 27, Jurensismergel Formation, ?Thouarsense Zone. GZG.INV.873: d = 40 mm, di = (27) mm, u = 11 mm, wh = 18 mm, wb = 9.5 mm, rb/2 = 20.

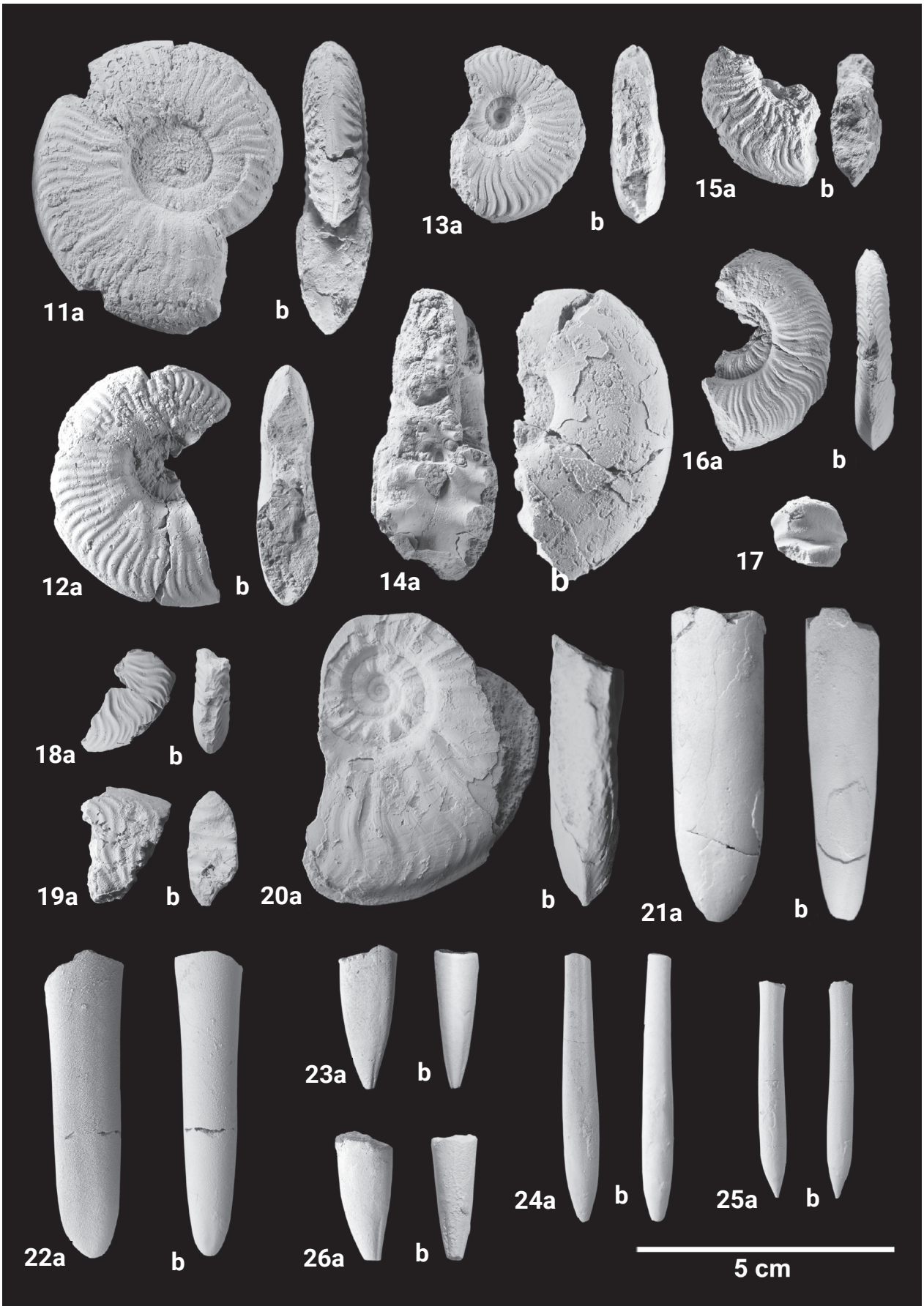
11a
b
13a
b
15a
b
12a
b
14a
b
16a
b
17
18a
b
19a
b
20a
b
21a
b
22a
b
23a
b
24a
b
25a
b
26a
b
5 cm

Figures 11–26. Ammonites and Belemnites of the Upper Toarcian of the Hainberg section **11.** *Phlyseogrammoceras dispansiforme* (Wunstorf), bed 28 "zeta conglomerate", Jurensismergel Formation, Dispansum Subzone. GZG.INV.874: d = 55.5 mm, di = (38) mm, u = 17 mm, wh = 24 mm, wb = 14 mm, rb/2 = (30); **12.** *Phlyseogrammoceras dispansiforme* (Wunstorf), bed 28 "zeta conglomerate", Jurensismergel Formation, Dispansum Subzone. GZG.INV.875: d = 49.5 mm, di = 34.5 mm, u = 13 mm, wh = 23.5 mm, wb = 13 mm, rb/2 = 31; **13.** *Phlyseogrammoceras transiens* (Ernst), bed 28 „zeta conglomerate", Jurensismergel Formation, Dispansum Subzone. GZG.INV.876: d = 34 mm, di = (23) mm, u = 9.5 mm, wh = 15.5 mm, wb = 10 mm, rb/2 = 24; **14.** ?*Alocolytoceras* sp., bed 28, Jurensismergel Formation, Dispansum Subzone. GZG.INV.877: d = (59) mm, wh = 28 mm, wb = 24 mm; **15.** *Cotteswoldia aalensis* (Zieten), bed 32, Opalinuston Formation, Aalensis Subzone. GZG.INV.878: d = (34) mm, wh = 17 mm, wb = 9 mm; **16.** *Pleydellia subcompta* (Branco), bed 32, Opalinuston Formation, Aalensis Subzone. GZG.INV.879: d = 40 mm, di = (28) mm, u = 15 mm, wh = 14.5 mm, wb = 18 mm, rb/2 = (45); **17.** Fragment of *Pleurolytoceras* cf. *hircinum* (Schlotheim), dorsal view showing v-shaped constriction; bed 32, Opalinuston Formation, Aalensis Subzone. GZG.INV.880; **18.** *Pleydellia* cf. *pseudoarcuata* Maubeuge, bed 39, Opalinuston Formation, Pseudolotharingicum Subzone. GZG.INV.881: wh = 11.5 mm, wb = 7 mm; **19.** ?*Cotteswoldia* sp., bed 39, Opalinuston Formation, Pseudolotharingicum Subzone. GZG.INV.882: wh= 20 mm, wb = 10 mm; **20.** *Leioceras* cf. *goetzendorfensis* (Dorn), Opalinuston Formation, Opalinum Subzone. GZG.INV.883: d = (70) mm, di = (48) mm, u = 19 mm, wh = 31 mm, wb = 14 mm; **21.** *Dactyloteuthis irregularis* (Schlotheim) [syn.: *Dactyloteuthis digitalis* (Blainville)], left: lateral view, right: dorsal view; bed 27, Jurensismergel Formation, ?Thouarsense Zone. GZG.INV.884: Length = 61 mm; **22.** *Dactyloteuthis similis* (Seebach), left: lateral view; right: dorsal view; bed 28, Jurensismergel Formation, Dispansum Subzone. GZG.INV.885: Length = 59 mm; **23.** *Acrocoelites rostriformis* (Theodori in Bronn) [syn.: *Acrocoelites* (*Odontobelus*) *curtus* (d'Orbigny)], left: lateral view, right: dorsal view; bed 32, Opalinuston Formation, Aalensis Subzone. GZG.INV.886: Length = 28 mm; **24.** *Hastites subclavatus* (Voltz), left: lateral view, right: dorsal or ventral view; bed 32, Opalinuston Formation, Aalensis Subzone. GZG.INV.887: Length = 52 mm; **25.** *Hastites subclavatus* (Voltz), left: lateral view, right: dorsal or ventral view; bed 32, Opalinuston Formation, Aalensis Subzone. GZG.INV.888: Length = 42.5 mm; **26.** *Acrocoelites rostriformis* (Theodori in Bronn) [syn.: *Acrocoelites* (*Odontobelus*) *curtus* (d'Orbigny)], left: lateral view, right: dorsal view; bed 39, Opalinuston Formation, Pseudolotharingicum Subzone. GZG.INV.889: Length = 24.5 mm.

ammonoids: *Cotteswoldia aalensis* (Zieten) (Fig. 15), *Pleydellia subcompta* (Branco) (Fig. 16), *Pleurolytoceras* cf. *hircinum* (Schlotheim) (Fig. 17); other fossils: *Hastites subclavatus* (Voltz) (Figs. 24-25), *Acrocoelites rostriformis* (Theodori in Bronn) (Fig. 23); *Nicaniella voltzii* (Hoeninghaus in Roemer), *Palaeonucula hammeri* (Defrance), fragments of *Chlamys textoria*, *Costatrochus subduplicatus* (d'Orbigny), *Thecocyathus mactrus* (Goldfuss), one terebratulid brachiopod, one serpulid tube, driftwood (jet);

Bed 33: 1 cm fibrous calcite with cone-in-cone structures;

Bed 34: 50 cm medium-grey, yellow-brown weathered, well-bedded claystone; few thin shell fragments, oxidized lenticular marcasite nodules; ca. 10 m lack of exposure (claystones);

Bed 35: 40 cm medium-grey, well-bedded claystone with abundant fine-grained white *Bositra* shell debris on bedding planes; fossils: *Bositra suessi* (Oppel) (one complete valve);

Bed 36: 5 cm medium-grey calcareous claystone with reworked cm-sized, rounded to irregular siderite concretions; top of concretions corroded and covered by thin veneer of echinoderm and bivalve debris; ammonoids: one reworked phosphoritic fragment of a ?*Cotteswoldia* sp.; other fossils: *Hastites* sp. (three fragments), pectinid bivalve fragments, small gastropods, one serpulid tube fragment;

Bed 37: 1 cm fibrous calcite with cone-in-cone structures;

Bed 38: 25 cm medium-grey, well-bedded claystone with fine-grained *Bositra* shell debris on bedding planes; fossils: *Coelodiscus minutus* (Schübler in Zieten) (limonite cast);

Bed 39: 1 cm yellow-brown calcareous clay with reworked phosphorite nodules, siderite nodule fragments, belemnites and phosphoritic ammonite fragments; ammonoids: *Leioceras*/*Pleydellia* sp. (fragment), *Pleydellia* cf. *pseudoarcuata* Maubeuge (Fig. 18) , ?*Cotteswoldia* sp. (Fig. 19); other fossils: *Acrocoelites rostriformis* (Theodori in Bronn) (Fig. 26);

Bed 40: 200 cm medium-grey, well-bedded claystone; 80 cm above basis a layer with fine-grained *Bositra* shell debris; 100 and 120 cm above basis 1-cm-thin siderite nodule beds;

Bed 41: >50 cm medium-grey, yellow-brown weathered unstratified clay (solifluction deposit) with white-grey septarian nodules; few marcasitic burrows and mica flakes; ammonoids: *Leioceras* cf. *goetzendorfensis* (Dorn) (Fig. 20).

Carbonate, organic carbon and sulphur contents

The Amaltheenton Formation (beds 1–6) is characterized by very low $CaCO_3$ contents (0.2 wt%) as well as low C_{org} contents (0.3–0.7 wt%) (Table 1, Fig. 2). Similarly, carbonate-free S_{tot} contents are low (0.3 wt%).

The lowermost Posidonienschiefer Formation (beds 7–9) is still very low in $CaCO_3$ (0.2 wt%) and C_{org} (0.7 wt%), despite the onset of lamination. Carbonate-free S_{tot} is even lower (<0.1 wt%) than in the Amaltheenton Fm. (Table 1, Fig. 2). Only at the base of the middle Posidonienschiefer Fm., i.e. in beds 10 and 11 (horizon of Elegantulum and Boreale Concretions) a marked increase in all three parameters ($CaCO_3$: 10 wt%, C_{org}: 22.1 wt%, carbonate-free S_{tot}: 1.9 wt%) can be observed. Carbonate-free C_{org} contents reach their maximum here with 24.7 wt%. Farther up in the middle Posidonienschiefer Fm. (beds 12 to 17), $CaCO_3$ contents remain comparatively high (around 52 wt%). Likewise, C_{org} and carbonate-free S_{tot} fluctuate at elevated val-

Figure 27. Limestone concretion ("Elegantulum Concretion") of bed 10 with *Lepidotes elvensis* (de Blainville) and *Eleganticeras elegantulum* (Young & Bird). GZG.INV.890ab: d = 28.7 mm, u = 8 mm, wh = 12 mm, wb = 7.8 mm.

ues (around 10 and 1.8 wt%, respectively). Normalised to the carbonate-free fraction, beds 16 and 17 again show similarly high C_{org} contents (around 23 wt%) as in beds 10 and 11. A cyclicity of the C_{org} contents, indicated by maxima in beds 10, 12, 16 and 17 with subsequent decreases, is unfortunately not provable due to the too low sample density. Beds 18–23, which include the "Monotis event bed" and "Commune Belemnite Battlefield", again show increased $CaCO_3$ contents (around 60 wt%) and high carbonate-free S_{tot} contents (around 2.1 wt%), but with tending declines in carbonate-free C_{org} (from about 20 to 10 wt%).

The upper part of the Posidonienschiefer Fm., represented by beds 24–26, is characterised by only moderately high $CaCO_3$ contents (around 27 wt%) and consistently high carbonate-free S_{tot} contents (around 2.1 wt%), with C_{org} and carbonate-free C_{org} stabilising at values around 10 and 13.5 wt%, respectively. The uppermost, bioturbated bed 26 of the Posidonienschiefer Fm., however, already shows significantly reduced C_{org} (2.4 wt%) and S_{tot} contents (<0.1 wt%).

The Jurensismergel Formation with its strongly condensed, bioclastic and Fe-oolitic rocks (beds 27–29) shows clearly elevated $CaCO_3$ contents (up to 66 wt%) with now very low C_{org} (around 1 wt%) and S_{tot} (below 0.1 wt%) (Table 1, Fig. 2). Only the basal belemnite accumulation is still characterised by high S_{tot} contents (1.5 wt%, i.e., 2.3 wt% carbonate-free S_{tot}).

The Opalinuston Formation (beds 31–41) is composed of only slightly calcareous mudstones, with significant lower $CaCO_3$ values (around 2.0 wt%) compared to the Jurensismergel Fm. rocks, but slightly higher than the Amaltheenton Fm. rocks (0.2 wt%). Only the stromatolite-bearing condensed bed 32 and the conglomeratic bed 36 show increased $CaCO_3$ contents of 44 and 23 wt%, respectively. C_{org} and S_{tot} contents of the Opalinuston Fm. (total rock as well as carbonate-free fraction) are only 0.9 wt% and 0.3 wt%, respectively (Table 1, Fig. 2).

Belemnite accumulations

The orientation of the tip direction of belemnite rostra was measured in bed 23 ("Commune Belemnite Battlefield") of the Posidonienschiefer Formation and bed 27 ("Oolite marl with belemnite accumulation") of the Jurensismergel Formation (Suppl. material 1).

In bed 23, a total of 79 rostra with a length between 1 and 9 cm were analysed. The belemnite rostra tip direction pattern shows one maximum in the class 195–210° (i.e., 10.1%), a second and third maximum in the class 150–165° (i.e., 8.9%) and 105–120° (i.e., 8.9%). The average azimuth of all measurements is 156° (Fig. 28).

In bed 27, a total of 104 rostra with a length between 1 and 9 cm were analysed. While there is one maximum at 165–180° (i.e., 9.6%), several further maxima occur at 45–60° (i.e., 7.7%), 0–15° (i.e., 6.7%), 30–45°, 60–75°, 90–105°, 285–300°, and 300–315° (each 5.8%). The average azimuth of all measurements for bed 27 is 86° (Fig. 29).

Stromatolites

Up to 9 mm thick laminated, sulphide-rich stromatolitic carbonate crusts were detected on cm-sized ammonite shell fragments in bed 32 of the Opalinuston Formation (Fig. 30). The crusts are composed of slightly undulating to flat hemispheroids. Thin sections demonstrate that the lamination results from an alternation of 10–40 µm thick microcrystalline to microsparitic and 15–40 µm thick dark, iron-sulphide-rich layers (Fig. 30). The stromatolitic crusts neither show a fenestral fabric nor morphological traces of microbial filaments or coccoidal structures. The same type of stromatolites has been described from discontinuities in the South-German Schwarzjura-Group by Keupp and Arp (1990).

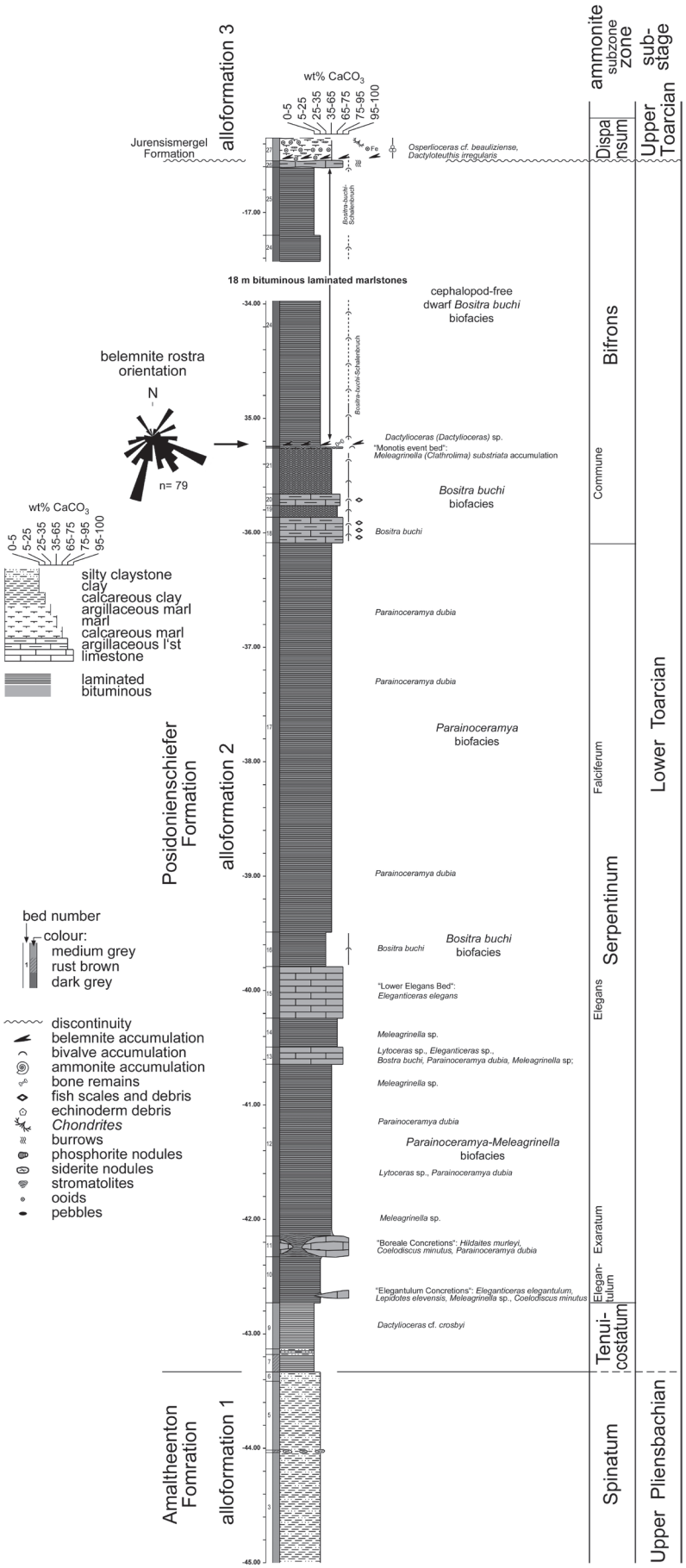

Figure 28. Lithostratigraphy, biostratigraphy and biofacies of the Posidonienschiefer Formation, Lower Toarcian, exposed at the Hainberg section.

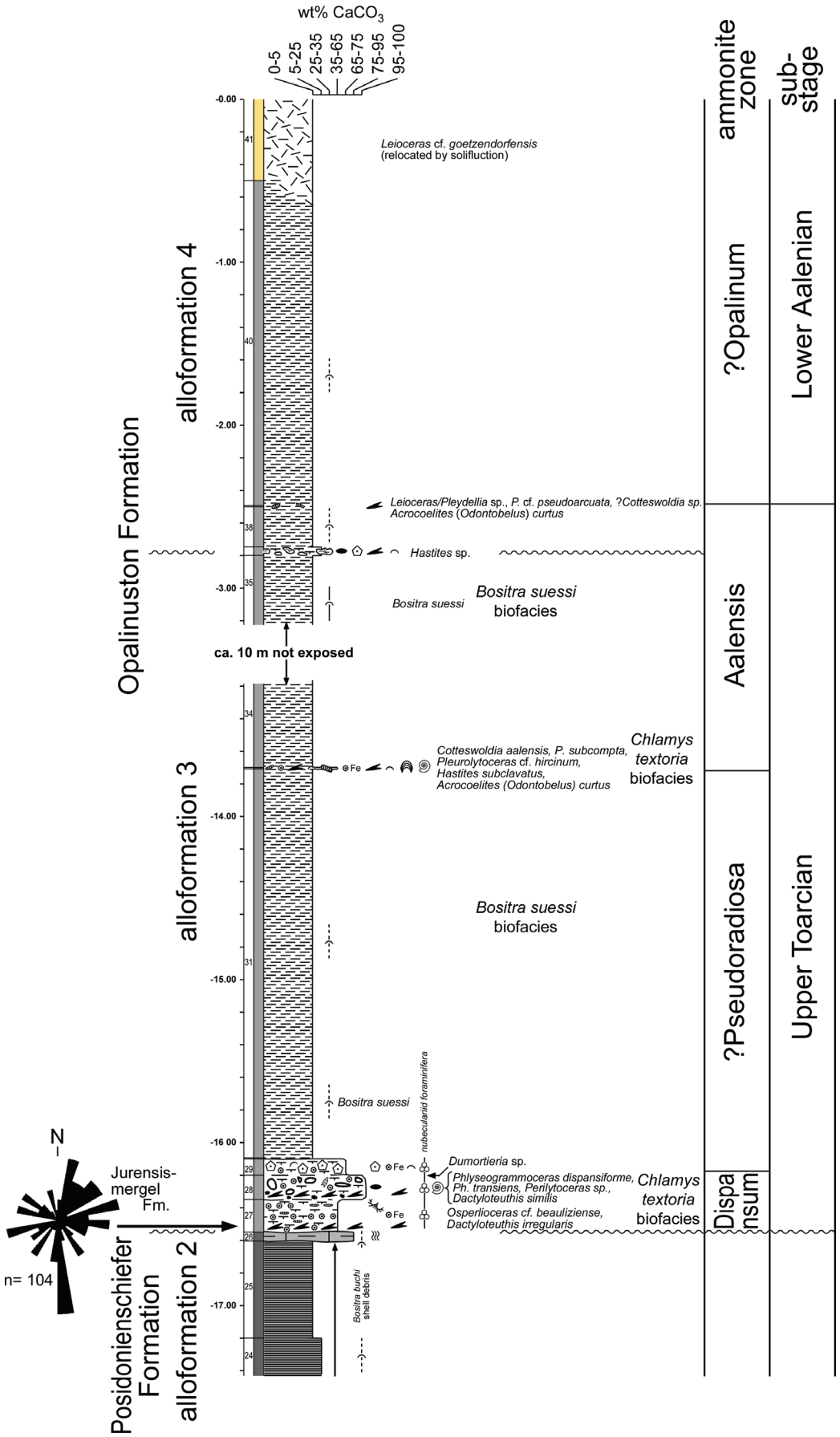

Figure 29. Lithostratigraphy, biostratigraphy and biofacies of the Jurensismergel Formation, Upper Toarcian, exposed at the Hainberg section. For legend see Fig. 28.

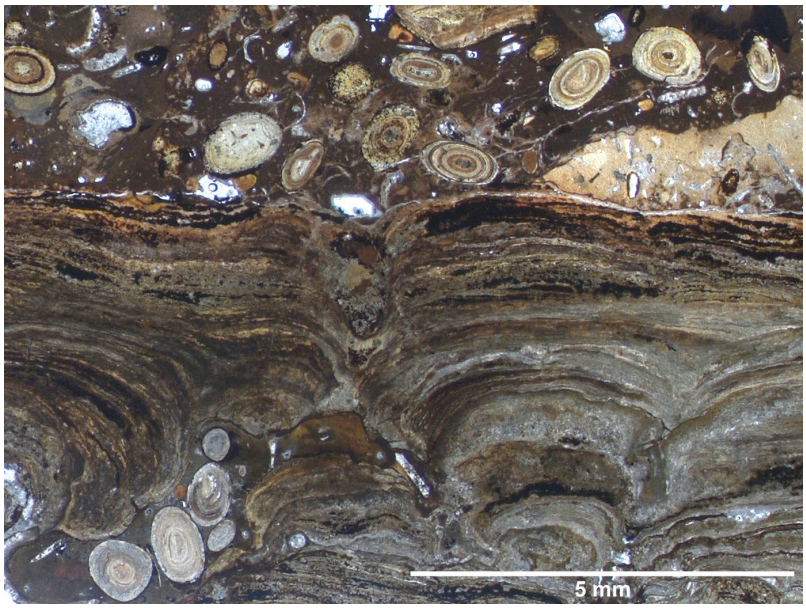

Figure 30. Thin section micrograph of a stromatolite crust of bed 32, Mactra/Aalensis Subzone, accompanied by marlstone with ooids showing mixed limonitic-calcareous cortices. Note the very dense lamination lacking a fenestral fabric and morphological microbial remains.

Bivalve assemblages

Although quantitative bivalve samples were not collected, qualitative descriptions provide some information on the general development of bivalve assemblages for the Toarcian along the section (Figs 28, 29; Suppl. material 2). No bivalves were recovered from the top parts of the Amaltheenton Fm. (beds 1–6) and lowermost parts (beds 7–9) of the Posidonienschiefer Fm. (i.e., gap of collection).

Lower parts of the middle Posidonienschiefer Fm. (beds 10–14) are dominated by *Parainoceramya dubia* (Sowerby) and *Meleagrinella* (*Clathrolima*) sp., which regularly occur on bedding planes. This "*Parainoceramya Meleagrinella* biofacies" is associated with cephalopods. Only in bed 13, first *Bositra buchi* (Roemer) covering single bedding planes were observed.

Further up in the middle Posidonienschiefer Fm., bed 16 is characterized by abundant bedding planes covered with *Bositra buchi* (Roemer) ("*Bositra buchi* biofacies"), while bed 17 regularly shows *Parainoceramya dubia* (Sowerby) but lacking *Bositra*. Beds 18–21 again show abundant bedding planes covered with *Bositra buchi* (Roemer) ("*Bositra buchi* biofacies"). The dense shell package results in a wrinkled pseudo-lamination of the rock.

Almost at the top of the middle Posidonienschiefer Fm., a monospecific *Meleagrinella* (*Clathrolima*) *substriata* (Münster) mass accumulation is developed, i.e. the "Monotis event bed" 22. Cephalopods are still present in this part of the section (Fig. 28).

Finally, the upper parts of the Posidonienschiefer Fm. (beds 24–25) are characterized by abundant beddings planes with *Bositra buchi* (Roemer) of reduced size (max. 6 mm) and its shell debris. Except for the immediate basis, this section is devoid of cephalopods ("cephalopod-free dwarf *Bositra buchi* biofacies") (Fig. 28).

After a stratigraphic gap, iron-oolitic marls (beds 27–28) of the Jurensismergel Formation commonly show valves of the epibyssate *Chlamys textoria* (Schlotheim), associated with scattered *Parainoceramya* sp., *Liostrea erina* (d'Orbigny) and rare *Palaeonucula hammeri* (Defrance) ("*Chlamys textoria* biofacies"), while claystones of the lower Opalinuston Formation are characterized by *Bositra suessi*, locally forming accumulations on bedding planes ("*Bositra suessi* biofacies"; Fig. 29). Further up in the Opalinuston Formation, *Bositra buchi* (Roemer) significantly decreases in abundance.

Discussion

Litho- and allostratigraphy

Distinct lithofacies changes, marker beds and discontinuities provide a good allostratigraphic framework, which partly corresponds to lithostratigraphic formations (Figs 2, 28, 29). The application of the terms "formation" and "alloformation" follows the recommendations in NACSN (1983, 2021), Lutz et al. (2006) and Pratt et al. (2023):

Alloformation 1 (equivalent to Amaltheenton Formation): Bedded medium-grey claystones with mica and silt-layers (beds 1–6) represent the top parts of the Amaltheenton Formation.

Alloformation 2 (equivalent to Posidonienschiefer Formation): The onset of fine-laminated medium-grey, rust-brown weathered claystones (beds 7–9) represents the lower boundary of the Posidonienschiefer Formation with its 60 cm thick lower, still non-bituminous part. An increase to high C_{org} values, marking the onset of the middle Posidonienschiefer Fm. with the T-OAE, is observed in bed 10. This 7.48 m thick middle, bituminous, part of the Posidonienschiefer

Fm. comprises beds 10 to 23, i.e. includes the Monotis event bed 22 and Commune Belemnite Battlefield (bed 23) at its top. The following upper part of the Posidonienschiefer Fm. (beds 24–26) consists of a 18.66 m thick monotonous succession of laminated bituminous marls with small *Bositra buchi* (Roemer) as almost the only fossils. The C_{org} contents are slightly lower than in the middle Posidonienschiefer Fm., similar to the trends in Southern Germany (Frimmel et al. 2004; Arp et al. 2021), but different from results in the Braunschweig area (Brockamp 1944). The top bed of the alloformation 2 is formed by bed 26, which is a laminated concretionary bed with distinct, straight burrows. This bed is considered as an equivalent of the "fucoid bed" at the top of the Posidonienschiefer Formation in Southern Germany (see e.g. Riegraf et al. 1984; Riegraf 1985). No deposits of the Dörnten Subformation with their fossiliferous limestone concretions were detected, consistent with former observations of Denckmann (1892: p. 107).

Alloformation 3 (corresponds to Jurensismergel and lowermost Opalinuston Formations): After a sharp boundary and discontinuity, the Jurensismergel Formation starts with a Fe-oolitic marls with a basal belemnite accumulation followed by a conglomeratic, Fe-oolitic calcareous clay bed with a second belemnite accumulation at its basis, and an echinoderm debris bed at its top. This rather marly, condensed and fossiliferous part of the Jurensismergel Fm. (beds 27–29) shows only 45 cm thickness. The higher, 13.3 m thick parts of this alloformation (beds 30–35) comprise medium-grey, bedded claystones, with more or less abundant *Bositra suessi* debris. This lithology already represents the Opalinuston lithofacies, so that earlier authors already assigned these beds in this region to the "Schichten des *Am. opalinus*" (von Seebach 1864), "Untere Zone des *Ammonites opalinus*" (Brauns 1865), or "Thone des *Harp. opalinum*" (Denckmann 1892). The thin bed 32 with reworked phosphorites and stromatolite crusts points to a minor discontinuity or condensation within this alloformation.

Alloformation 4 (corresponds to major parts of Opalinuston Formation): The lower boundary of this allostratigraphic unit is drawn with the erosional discontinuity of bed 36. Lithologically, the well-bedded carbonate-poor claystones are identical to those of the alloformation 3 top parts, except that *Bositra* shell debris layers are scarce. Only the lowermost 2.8 m of this formation were exposed.

Biostratigraphy

Only a limited number (24) of determinable ammonites were recovered from the investigated section (Figs 3–26). A number of them were compressed and poorly preserved. However, well-preserved uncompressed specimens have been found in limestone concretions in the Posidonienschiefer Fm. and phosphorite-bearing beds of the Jurensismergel and Opalinuston Formations. For the biostratigraphic scheme of ammonite zones and subzones, the reader is referred to Gabilly 1976a, Knitter and Ohmert 1983; Riegraf et al. 1984; Riegraf 1985; Ohmert et al. 1996; Elmi et al. 1997, and Cresta et al. 2001, summarized in Arp et al. (2021).

Upper Pliensbachian: Top parts of the alloformation 1 (≙ Amaltheenton Fm.) are devoid of biostratigraphic relevant fossils in the investigated section, but *Pleuroceras spinatum* has been recovered from a former clay pit near Sillium 1.5 km NNW of the investigated section (specimen in BGR collection: BGR-H-STGR-000290034 and -000290039; leg. R. Jordan 1956). The youngest, *in situ* collected *Pleuroceras spinatum* in this region comes from an 1.85 m thick interval at the top of the Amaltheenton Formation of the Friederike Mine near Bad Harzburg (Jordan 1960: his Abb. 14). No findings at the immediate lithostratigraphic boundary Amaltheenton-Posidonienschiefer are known. The precise boundary to the Toarcian, therefore, cannot be drawn with confidence.

Lower Toarcian: The lowermost recovered ammonite from alloformation 2 (≙ Posidonienschiefer Fm.), a poorly preserved, compressed *Dactylioceras* cf. *crosbeyi* (Simpson) with low umbilical width in bed 9 points to the presence of the Tenuicostatum Zone (Figs 3). Unfortunately, the Siemensi and Capillatum Concretions of the Tenuicostatum Zone, elsewhere present in this region (Wunnenberg 1950; Hoffmann 1968a, b; Weitschat 1973), are not developed at the investigated site. Their absence, however, rather reflects different early diagenetic conditions in the former porewater, not a stratigraphic gap (Hoffmann 1968b: p. 20). Clear evidence for the Tenuicostatum Zone, therefore, can only be given by *Dactylioceras semicelatum* (Simpson) from Heinde (BGR collection, e.g., BGR-H-STGR-000292526) and Haverlah (Hoffmann and Martin 1960), both locations with well developed limestone concretions. One *Dactylioceras* sp. is mentioned from 22–29 cm above basis of the Posidonienschiefer Formation, Friederike Mine near Bad Harzburg (Jordan 1960: p. 109). *Eleganticeras elegantulum* (Young & Bird) within the limestone nodule of bed 10 (Elegantulum Concretions; Fig. 27) indicates the Elegantulum Subzone, i.e. the basis of the Serpentinum Zone. The limestone nodules of bed 11 (Boreale Concretions) show well-preserved, uncompressed *Hildaites murleyi* (Moxon) (Fig. 4), indicating the Exaratum Subzone, while bed 15 (Lower Elegans Bed) belongs to the Elegans Subzone due to findings of compressed *Eleganticeras elegans* (Sowerby) (Fig. 6). The following beds 16 and 17 did only reveal indeterminable fragmentary imprints of *Harpoceras* sp. and likely represent higher parts of the Serpentinum Zone, while beds 18–21 probably already belong to the basal Bifrons Zone. No ammonite findings were made in these beds 18–21 of the present section.

However, Vinken (1971, p. 61 f.) provides a partial section from Listringen (9 km WNW of the Hainberg section), showing the "interval of Monotis limestones" (i.e., bituminous calcareous marls with wrinkled lamination due to *Bositra* and *Meleagrinella* shells) with a basal limestone bed containing *Dactylioceras commune* (Sowerby) and ?*Frechiella subcarinata* (Young & Bird) (Suppl. material 3). This bed corresponds to bed 18 of the Hainberg section.

Differing from that, Riegel et al. (1986) and Loh et al. (1986) draw the lower boundary of the Bifrons Zone

at Hildesheim-Itzum (Suppl. material 4) several meters deeper, which corresponds approximately to the middle of bed 17 in the Hainberg section. They support their stratigraphic assignment by the replacement of *Harpoceras* by abundant *Dactylioceras* in their section. However, the genus *Dactylioceras* occurs throughout the Posidonienschiefer Fm. in varying abundances. Many of these dactylioceratids cannot be attributed with confidence to a specific species if compressed (such as *D. commune* of the Bifrons, and *D. toxophorum* Buckman of the Serpentinum Zone), a fact already noted by Hoffmann (1968a, p. 452). The identification of the basis of the Bifrons Zone, therefore, appears more reliable using *Frechiella subcarinata* (Young & Bird), which appears identifiable even if compressed or less well preserved.

Indeed, Weitschat (1973) places the boundary Serpentinum-Bifrons zone in the lower part of the "interval of Monotis limestones" (which he defines as a 0.4–1.0 m thick interval of bituminous limestone beds partially with left valves of *Meleagrinella* (*Clathrolima*) *substriata* (Münster)), because of a *Harpoceras falciferum* (Sowerby) [not figured] finding within the "basal Posidonia pavements". This bed corresponds to our bed 18 in the Hainberg section. It has to be noted, however, that *Harpoceras falciferum* (Sowerby) reaches into the Commune Subzone (Howarth (1992, p. 132 and text-figs. 2, 5 and 6), thus, overlaps with *Dactylioceras commune* (Sowerby) and *Frechiella subcarinata* (Young & Bird). We therefore place the basis of the Bifrons Zone, Commune Subzone at the basis of bed 18 in the Hainberg section.

In the present investigation, poorly preserved *Dactylioceras* (*Dactylioceras*) sp. were only found in the "Commune Belemnite Battlefield" (bed 23) and at the very basis of the upper Posidonienschiefer Fm. (i.e., near the lower boundary of bed 24; Fig. 7). No further ammonites were found in beds 24–26. Likewise, no ammonite findings are reported from the upper Posidonienschiefer Fm. in adjacent sections Haverlahwiese and Hildesheim-Itzum. While the presence of the Fibulatum Subzone is likely (*Hildoceras bifrons* (Bruguiere) from Dörnten; Ernst 1923–1924), the presence of the Semipolitum Subzone appears questionable.

Upper Toarcian: No indication of the Variabilis Zone was found at the Hainberg section, consistent with its absence already shown by Denckmann (1892) and similar to adjacent sections Haverlahwiese and Hildesheim-Itzum (Maul 1984; Loh et al. 1986; Riegel et al. 1986). However, the Variabilis Zone, which forms major parts of the Dörnten Subformation, is well documented in Dörnten and Gallberg (Denckmann 1892; Ernst 1923–24; Dahlgrün 1928). It is probably present at the city centre of Hildesheim (Bischofskamp), from which Denckmann (1892) reports "*Harp. quadratum* Quenst. und *Harp. bingmanni* Denckm." in the collection of the Roemer-Museum Hildesheim) (Fig. 32).

The stratigraphically lowest ammonite finding of alloformation 3 (≙ Jurensismergel and lowermost Opalinuston Formations) at Hainberg, an *Osperleioceras* cf. *beauliziense* (Monestier) in bed 27 ("oolite marl"; Fig. 10), points to the Fallaciosum Subzone (Lacroix and Le Pichon 2011). The specimen is probably reworked into the Dispansum Zone, although the latter cannot be proven for the bed 27 directly. Unfortunately, the belemnite *Dactyloteuthis irregularis* (Schlotheim) (Fig. 21), abundant in bed 27, also does not provide a precise biostratigraphic assignment, because it ranges from the Variabilis Zone into the Pseudoradiosa Zone (Kolb 1942; Riegraf 1996; Schlegelmilch 1998; Weis 1999; Arp 2010).

A clear assignment of bed 28 ("zeta conglomerate") to the Dispansum Zone was possible due to findings of well preserved *Phlyseogrammoceras dispansiforme* (Wunstorf) (Figs 11, 12) and *Phlyseogrammoceras transiens* (Ernst) (Fig. 13). The single finding of a ?*Alocolytoceras* sp. (Fig. 14) is consistent with this interpretation. Similarly, the co-occurring belemnite *Dactyloteuthis similis* (Seebach) (Fig. 22) is consistent with the Dispansum Zone (Kolb 1942; Riegraf 1996). One poorly preserved *Dumortieria* sp. at the top of bed 28 indicates the transition to the Pseudoradiosa Zone. Bed 31, forming the lowermost parts of the Opalinuston Formation, unfortunately revealed only indeterminable compressed ammonoids and may represent younger parts of the Pseudoradiosa Zone.

However bed 32, with reworked phosphorite nodules, some ooids, stromatolite crusts and abundant belemnites, clearly represents a condensed lowermost part of the Aalensis Zone due to findings of *Cotteswoldia aalensis* (Zieten) (Fig. 15), *Pleydellia subcompta* (Branco) (Fig. 16), *Pleurolytoceras* cf. *hircinum* (Schlotheim) (Fig. 17), *Hastites subclavatus* (Voltz) (Figs 24, 25) and *Acrocoelites rostriformis* (Theodori in Bronn) (Fig. 23). The following 10 m gap of exposure and beds 34 to 35 probably still represent the Aalensis Subzone.

While only few fragmentary ammonoid remains (Figs 18, 19: *Pleydellia* cf. *pseudoarcuata* Maubeuge, ?*Cotteswoldia* sp.) were recovered from beds 36–41 of alloformation 4 (≙ major parts of Opalinuston Formation), *Acrocoelites rostriformis* (Theodori in Bronn) from bed 39 (Fig. 26) indicates that this bed is still Upper Toarcian in age. This belemnite species is known to occur from the uppermost Pseudoradiosa Zone (i.e. Moorei Subzone) to the top of the Aalensis Zone (Riegraf 1996; Rulleau 2007), if its short variety "*Acrocoelits curtus* (d'Orbigny)" (e.g. Arp 2010) is included in this taxon. Pinard et al. (2014) indicate its range into the lowermost Opalinum Zone, but the assignment of corresponding findings (Dumortier and Fontannes 1876; Quenstedt 1845–1849) cannot unequivocally assigned to the Aalensis or Opalinum Zone.

Lower Aalenian: Clear indication of Lower Aalenian provides *Leioceras* cf. *goetzendorfensis* (Dorn) (ex *Leioceras comptum* (Reinecke); see Dietze et al. 2021) from nodules of bed 41 at the top of the Hainberg section (Fig. 20), which is affected by solifluction. The ammonite, therefore, probably originates from further up in the section. *In situ* evidence for the Opalinum Subzone has not been found at the Hainberg. *Leioceras opalinum* (Reinecke), however, has been mentioned from Dörnten by Brachmann (1991) and from Haverlahwiese, with several specimens are hosted in the collection of the BGR in Hannover (e.g., BGR-H-STGR-000241142; leg. Kolbe 1955, BGR-H-STGR-000241149: leg. R. Jordan 1958). Borgmann

(1990: p. 54, his Fig. 29) assigns a 15.4 m thick interval of claystones at Echte-Dögerode (30 km SSW of Hainberg) to the Opalinum Zone due to findings of *Leioceras opalinum lineatum* (Buckman). At Sehnde near Hannover, 30 km NNW of Hainberg, the Opalinum Zone is approximately 18 m thick (Hoffmann 1913).

In addition to the limited ammonite and belemnite findings discussed above, bivalve assemblages (Suppl. material 2) provide some supplementary information on the biostratigraphic position, when compared to the observations in Southern Germany (Röhl et al. 2001). The observations at Hainberg are also consistent with the distribution of bivalve assemblages mentioned in Maul (1984), Loh et al. (1986), and Riegel et al. (1986), except for *Steinmannia*, which has not been found at Hainberg. In Southern Germany, *Steinmannia radiata* (Goldfuss) is characteristic of the upper part of the Tenuicostatum Zone (Riegraf et al. 1984), i.e., and interval identical to the "*Bositra buchi* occurrence I" of Röhl et al. (2001).

With respect to the Serpentinum Zone (i.e., beds 10–17), bivalves are largely represented by *Parainoceramya dubia* (Sowerby) and *Meleagrinella* sp. As an intercalation, the *Bositra buchi* biofacies appears first in bed 16 of the Hainberg section, which corresponds to "occurrence II" of Röhl et al. (2001) in top parts of the Elegans Subzone in Dotternhausen. The *Bositra buchi* biofacies reoccurs in beds 18–21, which corresponds to the lower-middle Commune subzone in Dottenhausen (occurrence III of Röhl et al. 2001).

The Monotis event bed 22 corresponds to the Monotis bed in Southern Germany, i.e., a marker bed within Commune Subzone (Birzer 1936; Riegraf et al. 1984; Arp and Gropengießer 2016). From the sections Hainberg and Listringen it becomes clear that the Monotis event bed (i.e., the Monotis Bed s.str.) is located at the top of the "interval of Monotis limestones" sensu Weitschat (1973), which comprises a section of 40–100 cm thick shell-rich calcareous marls and marly limestones – possibly reflecting sediment condensation (Kaiser 2021). Finally, the cephalopod-free dwarf *Bositra buchi* biofacies is apparently time-equivalent to the *Bositra buchi* mass occurrence IV in Röhl et al. (2001) in the upper Commune and Fibulatum Subzones, however with cephalopods and normal-sized *Bositra* in Southern Germany. For the Upper Toarcian, with *Bositra suessi* dominating in bedded calcareous claystones and *Chlamys textoria* characterising condensed oolitic or conglomeratic beds, no ecostratigraphically relevant pattern has been recognized to date.

Sealevel changes and seawater currents

The investigated section Hainberg shows several discontinuities and condensed beds, separating continuous sediments with bedding or lamination, and beds with increased quartz silt and mica content (or even carbonaceous plant debris). Together with the biofacies and the comparison with sections along an offshore-coastal transect (Figs 1, 31), an interpretation of sequences controlled by sealevel changes can be made (Fig. 32). An important basis for comparison and discussion forms the sequence stratigraphic work of Zimmermann et al. (2015) for Northern Germany, as well as investigations from Southern Germany by Röhl and Schmid-Röhl (2005) and Arp et al. (2021) (Fig. 32). The transgressive-regressive sequences discussed here are considered to reflect changes in the shoreline trajectory, with the maximum regression surface at the end of a regression, and the maximum flooding surface at the end of a transgression (Embry and Johannessen 1992; Catuneau et al. 2009, 2011).

The Latest Pliensbachian sediments, i.e., the top of alloformation 1 (≙ Amaltheenton Formation) with quartz silt and mica, are considered as regressive, reflecting prograding siliciclastics of deltaic origin. This is in accordance with Zimmermann et al. (2015), who suggested a regression and mrs within Spinatum Zone. Seawater currents may have been directed from North to South, as indicated by the occurrence of cool water organisms (Arp and Seppelt 2012) and glendonites (Merkel and Munnecke 2023).

The following sequence boundary is located at or near the Amaltheenton/Posidonienschiefer Formation boundary, specifically within the lower Tenuicostatum Zone (Röhl and Schmid-Röhl 2005) or within the late Spinatum Zone (mrs Pli 2; Zimmermann et al. 2015). No sedimentological indication of a discontinuity is known from Hainberg and adjacent sections, so that a continuous sedimentation across the Pliensbachian-Toarcian transition appears likely. The lack of corresponding ammonites of the Paltum and Clevelandicum Subzones could reflect changing or reduced salinities during the lowstand conditions and proximity to deltaic influx.

For the 0.6 m thick Tenuicostatum and 6.6 m thick Serpentinum Zones, i.e. beds 7–17, a transgressive trend is indicated by first ammonites in bed 9, followed by ammonite-rich limestone concretions during the T-OAE (i.e., the negative $d^{13}C_{org}$ excursion in the Elegantulum and Exaratum Subzones; Hesselbo and Pieńkowski 2011; Xu et al. 2018) and continuing stagnant basin conditions with opportunistic bivalve assemblages during the Elegans and Falciferum Subzones (Röhl and Schmid-Röhl 2005).

Contrary to that, Zimmermann et al. (2015) suggest for the North-German Basin that this initial Toarcian transgression is followed by a maximum flooding surface (mfs Toa1) already within top parts of the Tenuicostatum Zone. This interpretation is based on a retrogradational shoreline shift of more than 200 km to the East (Zimmermann et al. 2015), with spreading of bituminous shale deposition to the Western Pomerania area (with *Dactylioceras* cf. *semicelatum*; Ernst 1967, 1991). Then, a regression from the latest Tenuicostatum to Bifrons Zone should follow, with the mrs Toa1 in the latest Bifrons Zone (Fig. 32).

Lowermost parts of the Bifrons Zone with the bivalve-shell-rich beds 18–22 (0.85 m "interval of Monotis limestones" sensu Weitschat 1973) can be interpreted as high-stand deposits with reduced rate of sedimentation (condensation according to Kaiser 2021), while the thin accumulation of *Meleagrinella* (*Clathrolima*) *substriata* (i.e., the Monotis bed s.str. at the top of this interval), trace-

able along 500 km to Southern Germany, is considered as an event bed (Arp and Gropengießer 2016). Indeed, Röhl and Schmid-Röhl (2005) place a mfs at the Serpentinum/Bifrons zone boundary in Southern Germany (Fig. 32).

The belemnite accumulation on top of the Monotis event bed, also known from the Franconian Alb, might reflect a SSE to NNW directed seawater bottom current though the "Hessian Seaway" (Fig. 1), after the possibly tectonic-induced "Monotis bed event" (Arp and Gropengießer 2016). Current-aligned belemnites have also been mentioned and figured at the same stratigraphic bed from the open pit mine Haverlahwiese by Hoffmann (1968a: p. 496, his pl. 34). Likewise, Maul (1984: p. 30) shows a rose diagram of 500 measurements from the Commune Belemnite Battlefield at Hildesheim-Itzum with a clear maximum at 165°, i.e., confirming a bottom current directed from SSE to NNW (Suppl. material 4). Later parts of the Bifrons Zone, i.e., the 18.66 m upper Posidonienschiefer Fm. (i.e., beds 24–26) with its cephalopod-free dwarf *Bositra* biofacies and increasing content of fine-grained mica and plant debris, is best explained as the regressive phase of a sequence (Fig. 32), with increasing terrestrial influx and decreasing salinities, in accordance with Zimmermann et al. (2015) and Röhl and Schmid-Röhl (2005). The lowering of carbonate-free C_{org} contents from the upper Falciferum (ca. 23 wt%) to the Bifrons Zone bituminous shales (about 13.5 wt%) reflects a dilution effect by the increased sedimentation rate. Anoxic bottom water conditions, therefore, continued unchanged in this region proximal to deltaic influx.

For the Upper Toarcian, a sequence stratigraphic interpretation remains difficult for the investigated section, because the absence of the Variabilis Zone and major parts of the Thouarsense Zone, a 10-m-lack of exposure, and limited ammonite findings. A preliminary interpretation, however, can be given on basis of the comparison with adjacent sections (Figs 31, 32).

A sealevel lowstand is inferred for the basis of the Variabilis Zone, i.e. just prior to the deposition of the Dörnten Subformation. The latter, while preserved in its type region and some basinal sections (e.g. Echte; Hoffmann 1968a), obviously has been eroded in the area Haverlahwiese-Hainberg-Hildesheim (except for Hildesheim-Bischofskamp: Denckmann 1892: p. 101).

Contrary to Southern Germany, there is apparently no significant erosional discontinuity within (Arp et al. 2021) or at the top of the Variabilis Zone (Riegraf 1985; Jordan and Schmidt-Kaler 1985), because the presence of all its subzones is evident by corresponding ammonite findings at Dörnten (Denckmann 1892; Ernst 1923–1924; Brachmann 1991). This might be related to higher subsidence and sedimentation rates in Northern Germany. Likewise, the Thouarsense Zone at Dörnten is proven by *Pseudogrammoceras doerntense* (Denckmann), *Ps. bingmanni* (Denckmann), *Ps. struckmanni* (Denckmann), and *Grammoceras striatulum* (Sowerby), with only the Fallaciosum Subzone absent (Fig. 32). Continuous sedimentation with bituminous shales from the Bifrons to Variabilis Zone is also likely farther North in Schandelah (van de Schootbrugge et al. 2019: p. 272; Visetin et al. 2022). The precise nature of the sedimentological boundary Posidonienschiefer s.str. to Dörnten Member (i.e., sharp or gradationally) is, however, unknown.

In any case, after the regressive top of the Bifrons Zone (i.e., the top of the Posidonienschiefer Formation with cephalopod-free dwarf *Bositra* biofacies), the change to a cephalopod biofacies (with ammonite-rich limestone concretions at Dörnten, Gallberg, and corresponding relics at Hildesheim-Bischofskamp) could best be explained by a transgression. Deviating from that, Zimmermann et al. (2015) suggests transgressive conditions only during the early Variabilis Zone, with a maximum flooding surface (mfs Toa2) within the latest Variabilis Zone (Fig. 32).

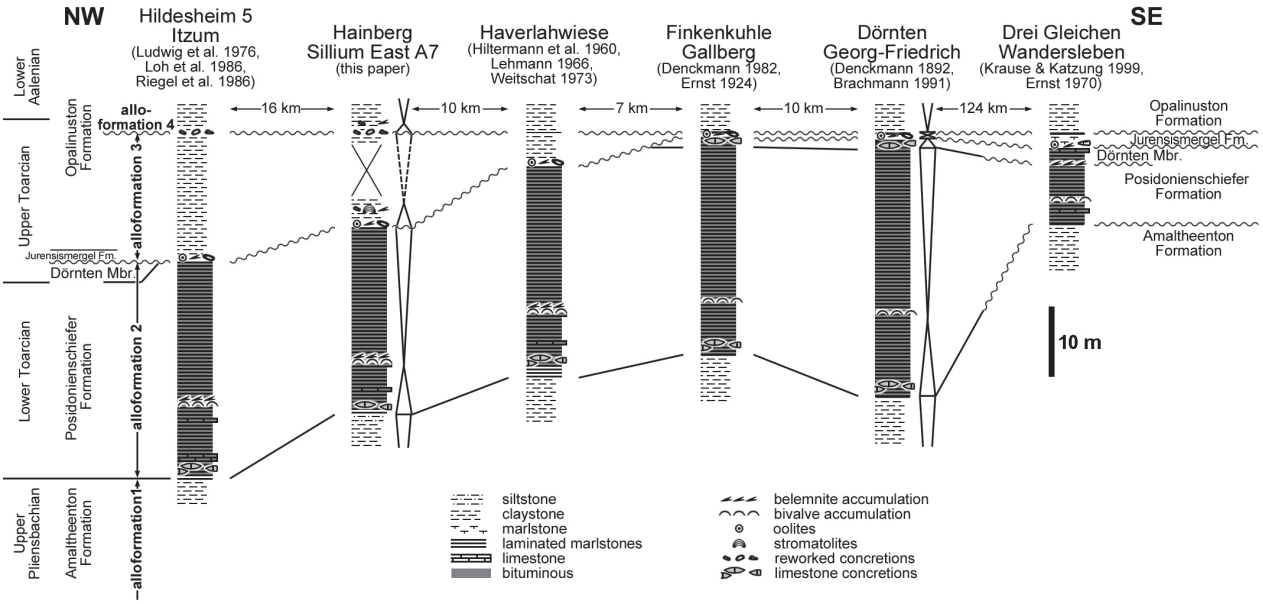

Figure 31. Correlation of the investigated section Hainberg with sections from Northern Germany and Thuringia, with suggested T-R cycles for the sections Hainberg and Dörnten.

The basis of the Dispansum Zone, i.e., the basis of alloformation 3, is the most obvious erosional sequence boundary in the working area, as indicated by conglomeratic oolitic marls and belemnite accumulations (i.e. beds 27–28) (Fig. 31). Indeed, submarine erosion removed the Variabilis and Thouarsense Zones as well as top parts of the Bifrons Zone in the area Haverlahwiese-Hainberg-Hildesheim, as already described by Denckmann (1892: p. 107). These conglomeratic deposits comprise reworked ammonites of the Variabilis and Thouarsense Zones (e.g. *Haugia* and *Grammoceras* sp. at Hildesheim-Itzum: Maul 1984; *Osperleioceras* cf. *beauliziense* (Monestier) at Hainberg), but are dominated by *Phlyseogrammoceras dispansum* (Lycett) and *Phl. dispansiforme* (Wunstorf), at least in their upper part (Hainberg). Unfortunately, no clear direction of potential bottom water currents was obtained from belemnite rostra alignment measurements (Fig. 29).

In accordance with that, Zimmermann et al. (2015) place their maximum regression surface mrs Toa2 within the latest Thouarsense Zone. Indeed, most of the described Jurensismergel Fm. sections in Northern Germany show a stratigraphic gap for the Fallaciosum Zone (Heidorn 1928), similar to Southern Germany, where a discontinuous Dispansum Zone belemnite accumulation overlies the Thouarsense Subzone with local erosion of the Fallaciosum Subzone (Arp et al. 2021). The conglomeratic-oolitic Dispansum Zone sediments themselves appear to be transgressive, with reworking at highly reduced siliciclastic influx.

The ongoing sealevel rise could be represented by strata dated to the Pseudoradiosa Zone, i.e., beds 29–31 of the Hainberg section. The condensed bed 32 with stromatolites might represent high-stand conditions, in analogy to the Pseudoradiosa/Aalensis zone transition in the Franconian Alb (Arp et al. 2021), if this correlation is correct. Unfortunately, the presence of this condensed bed has not yet been shown in adjacent sections due to limited detailed sedimentological observations (Fig. 31). Likewise, the following Aalensis Zone claystones (beds 34–35) are herein tentatively considered to represent a regressive phase. The discontinuity at bed 36 (i.e., the basis of alloformation 4), then possibly reflects a further sealevel lowstand and sequence boundary. Strikingly, a 1 m thick shelly carbonate bed has been reported from the Toarcian-Aalenian transition at Echte-Dögerode, 30 km SSW of the Hainberg (Borgmann 1990), where the Upper Toarcian is about 25 m thick (Hoffmann 1949, p. 122). Unfortunately, no definite ammonite proof of the presence and extent of the Pseudolotharingicum Subzone (i.e. top of Aalensis Zone) is available at the investigated section Hainberg. However, accepting *Acrocoelites rostriformis* (Theodori in Bronn) as an index fossil of the Upper Toarcian, the Pseudolotharingicum Subzone might cover the

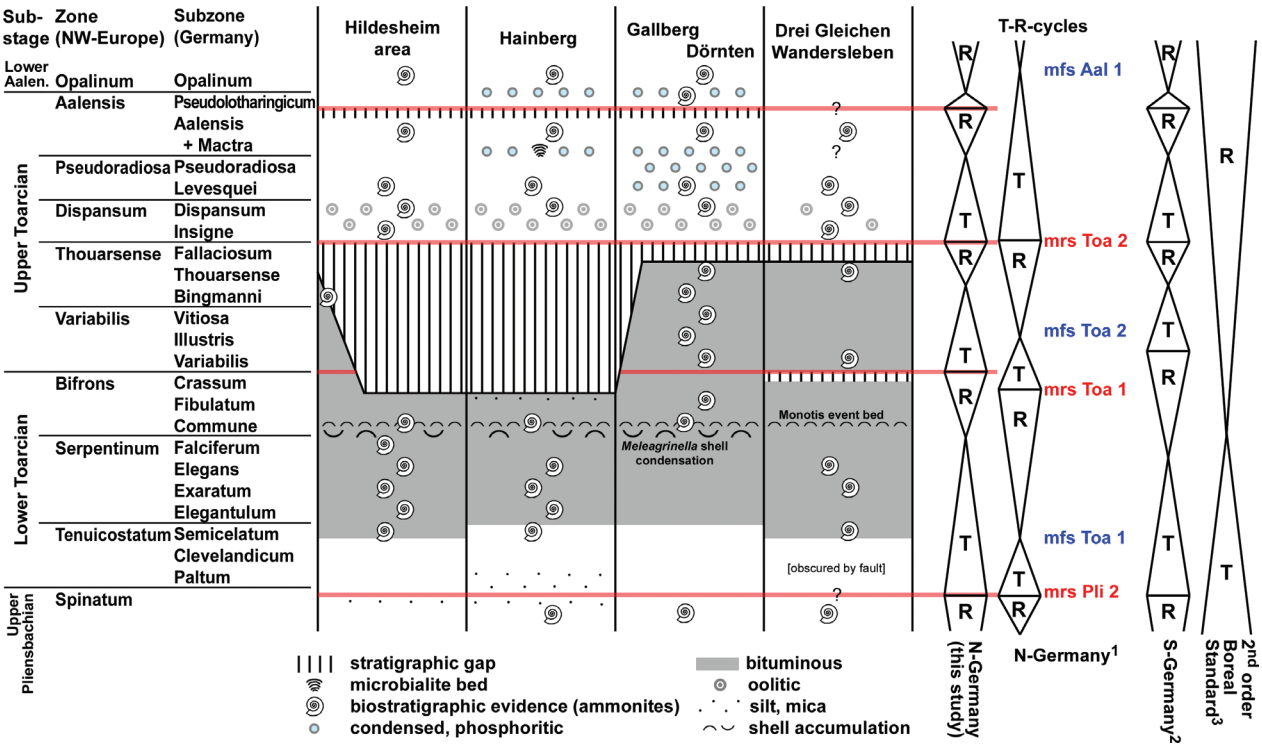

Figure 32. Sequence stratigraphic interpretation of the Toarcian succession in Northern Germany (including the Hainberg section) and Thuringia in comparison with 3rd order South-German and the 2nd order Boreal standard cycles. Sedimentary succession and ammonite biostratigraphic evidence according to Denckmann (1892), Ernst (1923–1924), Kumm (1941), Ernst (1970), Maul (1984), Brachmann (1991), Krause and Katzung (1999), and specimens from the BGR collection [https://gewis.bgr.de/, leg. K. Hoffmann, R. Jordan, K. Wiedenroth]. T-R cycles: [1] third order sequences Northern Germany (Zimmermann et al. 2015), [2] third order sequences Southern Germany (Röhl and Schmid-Röhl 2005; Arp et al. 2021); [3] second order sequences Boreal standard (de Graciansky et al. 1998; Jacquin et al. 1998).

thin transgressive interval of bed 38, followed by a condensed bed 39 and thicker regressive claystones (bed 40 and younger) of the Opalinum Zone. In any case, the sequence stratigraphic considerations on the Toarcian-Aalenian transition currently remain hypothetical and further complete sections with sufficient ammonite findings are required for testing and potential corrections.

Minor differences appear in the positions of maximum regression and maximum flooding surfaces between Toarcian sections of the central North-German Basin to Poland (Zimmermann et al. 2015), southern part of Northern Germany (this paper) and Southern Germany (Röhl and Schmid-Röhl 2005; Arp et al. 2021). These may reflect limitations of biostratigraphic high-resolution dating in the ammonoid-poor North-German deposits proximal to deltaic foresets, and corresponding interpolations in stratigraphic dating and correlation (Fig. 32).

Furthermore, the high thickness of sections in the Northern Germany and Poland (i.e. 82 to 231 m Toarcian for Usedom to Hamburg; Baermann et al. 2000; Zimmermann et al. 2015; e.g. ca. 90 m Toarcian at Nowa Wieś 12-Praszka 1/81: Pienkowski 2004) indicates significant higher subsidence and sedimentation rates, if compared to the Hainberg-Hildesheim area. Significantly increased clastic deposition (delta front and prodelta) during eustatic sealevel fall and (forced) delta progradation may have caused an apparent earlier onset of relative sealevel fall, if compared to the low subsidence and low sedimentation rate areas in Southern Germany. In turn, stratigraphic gaps covering intervals longer than subzones obscure the precise timing of maximum regression in areas of low subsidence, while ammonoid findings in thicker but more proximal positions are rare.

A further complication for interpreting thickness pattern and sedimentary sequences in the working area may result from possible synsedimentary ortho- and halotectonic movements during the Lower Jurassic at the Eichfeld-Altmark-High. Indeed, the available thickness data for alloformation 2 (Posidonienschiefer Fm. exclusive Dörnten Member) show short-distance variations between 29.7 and 33.4 m in the Hildesheim area, between 23.3 and 30.4 m at the Hainberg (unpublished drilling reports BGR), and between 30 and 37 m at the Salzgitter anticline (Gallberg: Ernst 1923–1924; Schröderstollen: Dahlgrün 1928) (Fig. 31). Larger thickness variations have been reported from the Hils Syncline (16 to 40 m; Littke and Rullkötter 1987), while the Braunschweig area shows rather uniform thickness pattern (Brockamp 1944) around 36.5 m (Schandelah; Visetin et al. 2022). For the lower and middle Posidonienschiefer Fm. a minor reduction in thickness is evident for the Hainberg, Haverlah and Gallberg sections, if compared to the Hildesheim area (NW) and Dörnten area (SE) (Fig. 31), as well as the Braunschweig area (Wunnenberg 1950; Visentin et al. 2022). These data, however, may rather point to minor local halotectonic movements or erosion at the top of the formation. Nonetheless, reduced thicknesses of 12 m at Wefensleben (67 km ENE of the Hainberg section; Koert 1923), possibly 3 to 7 m at Bad Harzburg (30 km SE of the Hainberg section; Kumm et al. 1941; Brockamp 1944), and 12–16 m in the Altmark area (Bauss 1976) may point to a structural zone of reduced subsidence farther East, i.e. the Eichsfeld-Altmark-High.

For alloformation 3 and 4 (i.e., Dörnten Member and Jurensismergel plus lower Opalinuston Fm.), spatial thickness pattern are even less well known due to poor outcrop conditions and difficulties in recognizing lithostratigraphic boundaries in drillings. Thus, the relation of condensed sections of these allostratigraphic units (e.g., in the Gallberg-Dörnten area) to structural elements remains to be investigated.

Conclusions

- Construction work at the A7 motorway cutting at the Hainberg, Lower Saxony, temporarily exposed a 40.81 m thick section of the Toarcian, with a 10 m gap within the Upper Toarcian Aalensis Zone.
- Above quartz silt bearing claystones of the Pliensbachian Amaltheenton Formation (alloformation 1), the 26.74 m thick Toarcian Posidonienschiefer Formation (alloformation 2) starts with 0.6 m laminated, C_{org}-poor claystones, followed by 6.6 m bituminous laminated marlstones with limestone beds, and the 0.85 m thick "interval of Monotis limestones". The C_{org} (carbonate-free) maximum of 24.5 wt% lies within the Elegantulum Subzone, while average C_{org} (carbonate-free) contents are about 19 wt%. The upper, 18.66 m thick part of the Posidonienschiefer Formation is characterised by varying, generally lower C_{org} contents (carbonate-free) around 13.5 wt%.
- Above an erosive discontinuity, the 13.76 m thick alloformation 3 comprises the 0.45 m thin Jurensismergel Formation with iron-oolitic marls including belemnite accumulations, and a 13.31 m interval (lowermost Opalinuston Formation) of C_{org}-poor carbonate clays with an intercalated ammonite condensation layer. The latter shows thin, non-cyanobacterial stromatolitic crusts. The boundary to the alloformation 4 (major parts of Opalinuston Formation) is drawn with an erosional layer of corroded geodes and echinoderm debris.
- With respect to biostratigraphy, ammonite findings indicate for the Lower Toarcian Posidonienschiefer Formation the presence of the Tenuicostatum Zone, Elegantulum-Subzone, Exaratum-Subzone, Elegans Subzone, and Commune Subzone. The presence and extent of the Falciferum Subzone is delimited by a first *Bositra buchi* maximum and the "interval of Monotis limestones". The upper Posidonienschiefer Formation is devoid of ammonites and might represent the late Commune and Fibulatum subzones. With respect to the Upper Toarcian Jurensismergel Formation, the Variabilis Zone is absent. One reworked *Osperleioceras* cf. *beauliziense* (Monestier) likely represents a relic of the Thouarsense Zone within thin condensed iron oolitic marls of the Dis-

pansum Zone at the discontinuous basis of the formation. The following calcareous claystones comprise the Pseudoradiosa and Aalensis zones, with their upper limit indicated by the last *Acrocoelites rostriformis* (Theodori in Bronn) in a thin layer of reworked fossils. Evidence for the Lower Aalenian, i.e. *Leioceras* cf. *goetzendorfensis* (Dorn), is found at the solifluction affected top bed of the section.

- With respect to sequence stratigraphy, three 3rd order transgressive-regressive cycles are recognized for the Toarcian succession in the investigated area, largely in accordance with previous studies in Northern (Zimmermann et al. 2015) and Southern Germany (Röhl and Schmid-Röhl 2005; Arp et al. 2021). After a regression during late Pliensbachian, a sequence boundary is evident at the Amaltheenton-Posidonienschiefer transition (mrs Pli 2 sensu Zimmermann et al. 2015). A transgressive phase is represented by the Elegantulum to Falciferum subzones, with highstand conditions and reduced sedimentation during Commune Subzone, superimposed by the Monotis bed event. A belemnite battlefield indicates seawater bottom currents from SSE. The corresponding regressive phase with increased sedimentation is developed during late parts of the Bifrons Zone. The cephalopod-free dwarf *Bositra* biofacies with increasing mica and plant debris reflects distant effects of prograding deltas and reduction of salinities. The following sequence boundary, not preserved at the site of investigation, is located at the Bifrons/Variabilis transition (mrs Toa 1 sensu Zimmermann et al. 2015).
  For the Upper Toarcian, the following tentative interpretation is given: The Variabilis to Thouarsense Zone represented by the Dörnten Member is likely a transgressive phase and highstand of the second Toarcian T-R cycle. The following regressive phase (Fallaciosum Subzone) is rarely preserved in Northern Germany. A major sequence boundary with significant erosion at Thouarsense-Dispansum zone boundary (mrs Toa 2 sensu Zimmermann et al. 2015) is associated with the removal of the Dörnten Member in the Hainberg-Hildesheim area. The following Dispansum Zone iron oolitic marls and Pseudoradiosa Subzone clays possibly form a transgressive phase of a third Toarcian T-R cycle, with highstand at the Pseudoradiosa-Aalensis zone transition. Aalensis Subzone claystones may represent the regressive phase, with a minor erosional sequence boundary at their top. The poorly delineated Pseudolotharingicum Subzone might be transgressive, with highstand condensations at its top, followed by a regressive phase of the Lower Aalenian Opalinum zone claystones.
- Minor deviations in the timely position of maximum flooding and regression surfaces between the different studies (Zimmermann et al. 2015; Röhl and Schmid-Röhl 2005; Arp et al. 2021) likely reflect effects of a higher subsidence at variable sedimentation rate in the North German Basin.

Acknowledgements

We thank Frank Wiese, Göttingen, for drawing our attention to the temporary outcrop during construction work at Sillium-East A7. The Lower Saxony State Authority for Road Construction and Transport, Bad Gandersheim, kindly gave the permission to investigate and sample the section at the motorway A7. Jochen Erbacher, BGR Hannover, kindly provided access to drilling reports of the BGR/LBEG. Thomas Wiese and Edgar Gandolph provided access to and gave support at the collection of the Federal Institute for Geosciences and Natural Resources (BGR), Hannover. Thin sections were prepared by Axel Hackmann, Göttingen. Accurate and helpful reviews by Volker Dietze, Nördlingen, and Matthias Franz, Göttingen, significantly improved the manuscript.

References

Althoff W (1936) Die Grenzschichten zwischen Lias und Dogger bei Bielefeld. - Zur Stratigraphie und Paläontologie des oberen Lias und unteren Doggers von Bethel bei Bielefeld. Abhandlungen aus dem Landesmuseum der Provinz Westfalen, Museum für Naturkunde 7(2): 11–45 [Münster].

Arnold H, Duphorn K, Meyer KD, Schneekloth H, Vinken R (1973) Geologische Übersichtskarte 1 : 200000, Blatt CC 3918 Hannover. BGR, Hannover. [1 map]

Arp G (2010) Ammonitenfauna und Stratigraphie des Grenzbereichs Jurensismergel/Opalinuston-Formation bei Neumarkt i.d. Opf. (oberstes Toarcium, Fränkische Alb). München. Zitteliana A50: 25–54. https://doi.org/10.5282/ubm/epub.11987

Arp G, Gropengießer S (2016) The Monotis-Dactylioceras Bed in the Posidonienschiefer Formation (Toarcian, southern Germany): condensed section, tempestite, or tsunami-generated deposit? Paläontologische Zeitschrift 90: 271–286. https://doi.org/10.1007/s12542-015-0271-7

Arp G, Seppelt S (2012) The bipolar bivalve *Oxytoma* (*Palmoxytoma*) *cygnipes* (Young & Bird, 1822) in the Upper Pliensbachian of Germany. Paläontologische Zeitschrift 86: 43–57. https://doi.org/10.1007/s12542-011-0113-1

Arp G, Gropengießer S, Schulbert C, Jung D, Reimer A (2021) Biostratigraphy and sequence stratigraphy of the Toarcian Ludwigskanal section (Franconian Alb, Southern Germany). Zitteliana 95: 57–94. https://doi.org/10.3897/zitteliana.95.56222

Baermann A, Kröger J, Taugs R, Wüstenhagen K, Zarth M (2000) Anhydritzemente im Rhätsandstein Hamburgs. Morphologie und Strukturen. Zeitschrift für Angewandte Geologie 46: 138–143. [Stuttgart]

Barnasch J, Franz M, Beutler G (2005) Hochauflösende Gliederung des Keupers der Eichsfeld-Altmark-Schwelle zur Präzisierung der Diskordanzen. Hallesches Jahrbuch für Geowissenschaften, B, Beiheft 19: 153–160.

Bauss R (1976) Zur Fazies und Paläogeographie des Toarc im Nordteil der DDR. Zentrales Geologisches Institut Berlin, unpublished report Nr. 61/76: 83 pp. [12 enclosures]

Birzer F (1936) Die Monotis-Bank in den Posidonien-Schiefern, besonders Frankens. Abhandlungen der Geologischen Landesuntersuchung am Bayerischen Oberbergamt 26: 3–32. [München]

Borgmann R (1990) Die Schichtenfolge an der Wende Lias/Dogger vom Kahlberg bei Echte (südliches Niedersachsen). Diploma Thesis Georg-August-Universität Göttingen, 153 pp.

Brachmann H (1991) Die Ammonitenfauna der „Dörntener Schichten" (Ober-Toarcium) von der Typlokalität bei Dörnten (N Harzvorland). Arbeitskreis Paläontologie Hannover 19: 88–115. [Hannover]

Brauns D (1865) Die Stratigraphie und Paläontographie des südöstlichen Theiles der Hilsmulde auf Grund neuer, bei den Eisenbahnbauten in den Jahren 1861–1864 angestellter Beobachtungen. Palaeontographica 13: 75–145.

Brockamp B (1944) Zur Paläogeographie und Bitumenführung des Posidonienschiefers im deutschen Lias. Archiv für Lagerstättenforschung 77: 7–59. [Berlin]

Brosche KU (1996) Wirkungen des pleistozänen kaltzeitlichen Klimas, insbesondere des Bodenfrostes, in den Sedimenten des östlichen Ostfalen (Raum Hannover-Wolfsburg-Helmstedt-Bad Harzburg-Salzgitter-Bad-Hannover) - Teil 1. E&G Quaternary Science Journal 46: 1–17. https://doi.org/10.3285/eg.46.1.01

Catuneanu O, Abreu V, Bhattacharya JP, Blum MD, Dalrymple RW, Eriksson PG, Fielding CR, Fisher WL, Galloway WE, Gibling MR, Giles KA, Holbrook JM, Jordan R, Kendall CGSC, Macurda B, Martinsen OJ, Miall AD, Neal JE, Nummedal D, Pomar L, Posamentier HW, Pratt BR, Sarg JF, Shanley KW, Steel RJ, Strasser A, Tucker ME, Winker C (2009) Towards the Standardization of Sequence Stratigraphy. Earth-Science Reviews 92: 1–33. https://doi.org/10.1016/j.earscirev.2008.10.003

Catuneanu O, Galloway WE, Kendall CGSC, Miall AD, Posamentier HW, Strasser A, Tucker ME (2011) Sequence stratigraphy: Methodology and nomenclature. Newsletters on Stratigraphy 44: 173–245. https://doi.org/10.1127/0078-0421/2011/0011

Cresta S, Goy A, Ureta S, Arias C, Barrón E, Bernad J, Canales ML, García-Joral F, García-Romero E, Gialanella PR, Gómez JJ, González JA, Herrero C, Martínez G, Osete ML, Perilli N, Villalaín JJ (2001) The Global Boundary Stratotype Section and Point (GSSP) of the Toarcian-Aalenian Boundary (Lower-Middle Jurassic). Episodes 24: 166–175. https://doi.org/10.18814/epiiugs/2001/v24i3/003

Dahlgrün F (1928) Das Profil des „Schroeder-Stollen" bei Dörnten und seine Bedeutung für die Tektonik des Salzgitterer Höhenzuges. Zeitschrift der deutschen geologischen Gesellschaft 79 (1927): 88–100.

Dahlgrün F (1939) Geologische Karte von Preussen und benachbarten deutschen Ländern. Lieferung 337. Erläuterungen zu Blatt Ringelheim Nr. 2159. 2nd edn., 64 pp. [Berlin (Preussische Geologische Landesanstalt)] [+1 map]

de Graciansky PC, Dardeau G, Dommergues JL, Durlet C, Marchand D, Dumont T, Hesselbo SP, Jacquin T, Goggin V, Meister C, Mouterde R, Rey J, Vail PR (1998) Ammonite biostratigraphic correlation and Early Jurassic sequence stratigraphy in France: comparisons with some U.K. sections. In: de Graciansky PC, Hardenbol J, Jacquin T, Vail PR (Eds) Mesozoic and Cenozoic Sequence Stratigraphy of European Basins, SEPM, Tulsa, 583–622. https://doi.org/10.2110/pec.98.60

Denckmann A (1887) Über die geognostischen Verhältnisse in der Umgegend von Dörnten nördlich Goslar, mit besonderer Berücksichtigung der Fauna des Oberen Lias. Abhandlungen zur geologischen Specialkarte von Preußen und den Thüringischen Staaten 8(2): 108 pp. [+ 10 plates]

Denckmann A (1892) Studien im Deutschen Lias. Bifrons-Zone und Dörntener Schiefer. Jahrbuch der Königlich Preussischen geologischen Landesanstalt und Bergakademie zu Berlin 13: 98–114.

Dera G, Donnadieu Y (2012) Modeling evidences for global warming, Arctic seawater freshening, and sluggish oceanic circulation during the Early Toarcian anoxic event. Paleoceanography 27: 1–15. https://doi.org/10.1029/2012PA002283

Di Cencio A, Weis R (2020) Revision of upper Toarcian ammonites (Lytoceratidae, Graphoceratidae and Hammatoceratidae) from the Minette ironstones, southern Luxembourg. Ferrantia 83: 5–103. https://ps.mnhn.lu/ferrantia/publications/Ferrantia83.pdf

Dietze V, Gräbenstein S, Franz M, Schweigert G, Wetzel A (2021) The Middle Jurassic Opalinuston Formation (Aalenian, Opalinum Zone) at its type locality near Bad Boll and adjacent outcrops (Swabian Alb, SW Germany). Palaeodiversity 14: 15–113. https://doi.org/10.18476/pale.v14.a3

Dorn P (1936) Paläogeographische Studien über das jurassische Posidonienschiefermeer Deutschlands. Tübinger naturwissenschaftliche Abhandlungen 15: 60. [+1 map]

Dumortier E, Fontannes F (1876) Description des ammonites de la zone à *Ammonites tenuilobatus* de Crussol (Ardèche) et de quelques autres fossiles jurassiques nouveaux ou peu connus. Mémoires de l'Académie de Lyon, Classe des Sciences 21: 162. [19 pls]

Duphorn K, Lang HD, Look ER, Mengeling H, Meyer KD (1974) Geologische Übersichtskarte 1 : 200000, Blatt CC 3926 Braunschweig. BGR, Hannover. [1 map]

Duyster JP (2000) StereoNett Version 2.46. Institut für Geologie, Ruhr-Universität Bochum.

Elmi S, Rulleau L, Gabilly J, Mouterde R (1997) Toarcien. In: Cariou E, Hantzpergue P (Coord.) Biostratigraphie du Jurassique ouest-européen et méditerranéen. Bulletin du Centre de Recherches Elf Exploration et Production, Mémoir 17: 25–36.

Embry AF, Johannessen EP (1992) T-R sequence stratigraphy, facies analysis and reservoir distribution in the uppermost Triassic-Lower Jurassic succession, western Sverdrup Basin, Arctic Canada. In: Vorren TO, Bergsager E, Dahl-Stamnes OA, Holter E, Johansen B, Lie E, Lund TB (Eds) Arctic Geology and Petroleum Potential, Vol. 2 (Special Publication). Norwegian Petroleum Society (NPF), 121–146. https://doi.org/10.1016/B978-0-444-88943-0.50013-7

Ernst W (1923–1924) Zur Stratigraphie und Fauna des Lias Zeta im nordwestlichen Deutschland. Palaeontographica 65(1923): 1–96. [plates 1–6]; 66 (1924): 97–222. [plates 7–14]

Ernst W (1967) Die Liastongrube Grimmen. Sediment, Makrofauna und Stratigraphie – Ein Überblick. Geologie 16(5): 550–569.

Ernst W (1970) Der Lias am NE-Abhang des Röhnbergrückens (südöstlich von Gotha). Geologie 19(4): 405–411.

Ernst W (1991) Der Lias im Ton-Tagebau bei Grimmen (Vorpommern). Fundgrube, Zeitschrift für Geologie, Mineralogie, Paläontologie und Bergbaugeschichte 27(4): 171–184.

Franz M, Arp G, Niebuhr B (2020) Schwarzjura-Gruppe. In: LithoLex [online data base]. Hannover, BGR. Last updated 30.01.2020 [cited 16.02.2020] Record no. 10000049. https://litholex.bgr.de

Frimmel A, Oschmann W, Schwark L (2004) Chemostratigraphy of the Posidonia Black Shale, SW Germany. I. Influence of sea-level variation on organic facies evolution. Chemical Geology 206: 199–230. https://doi.org/10.1016/j.chemgeo.2003.12.007

Gabilly J (1976a) Le Toarcien à Thouars et dans le central-ouest de la France. Les Stratotypes français 3: 217. [29 pls]

Heidorn F (1928) Paläogeographisch-tektonische Untersuchungen im Lias Zeta von Nordwestdeutschland. Neues Jahrbuch für Mineralogie, Geologie und Paläontologie, Beilage-Bände 59 (Abt. B): 117–244.

Hesselbo SP, Pieńkowski G (2011) Stepwise atmospheric carbon-isotope excursion during the Toarcian Oceanic Anoxic Event (Early Jurassic, Polish Basin). Earth and Planetary Science Letters 301: 365–372. https://doi.org/10.1016/j.epsl.2010.11.021

Heunisch C, Caspers G, Elbracht J, Langer A, Röhling HG, Schwarz C, Streif H (2017) Erdgeschichte von Niedersachsen – Geologie und Landschaftsentwicklung. GeoBerichte 6: 3–83. [Hannover (Landesamt für Bergbau, Energie und Geologie)]

Hiltermann H, Kolbe H, Schmid F (1960) Exkursion 1. Mesozoikum Niedersachsens. Paläontologische Zeitschrift 34: 3–6.

Hiss M, Mutterlose J, Niebuhr B, Schwerd K (2005) Die Kreide in der Stratigraphischen Tabelle von Deutschland 2002. Newsletters on Stratigraphy 41: 287–306. https://doi.org/10.1127/0078-0421/2005/0041-0287

Hoffmann G (1913) Stratigraphie und Ammonitenfauna des Unteren Doggers in Sehnde bei Hannover. Schweizerbart, Stuttgart, 201 pp. [18 pls]

Hoffmann K (1949) Zur Paläogeographie des nordwestdeutschen Lias und Doggers. In: Bentz A (Ed.) Erdöl und Tektonik in Nordwestdeutschland, Amt für Bodenforschung, Hannover, 113–129.

Hoffmann K (1968a) Die Stratigraphie und Paläogeographie der bituminösen Fazies des nordwestdeutschen Oberlias (Toarcium). Beihefte zum Geologischen Jahrbuch 58: 443–498.

Hoffmann K (1968b) Neue Ammonitenfunde aus dem tieferen Unter-Toarcium (Lias e) des nördlichen Harzvorlandes und ihre feinstratigraphische Bedeutung. Geologisches Jahrbuch 85: 1–32.

Hoffmann K, Martin GPR (1960) Die Zone des *Dactylioceras tenuicostatum* (Toarcien, Lias) in NW- und SW-Deutschland. Paläontologische Zeitschrift 34: 103–149. https://doi.org/10.1007/BF02987046

Howarth MK (1992) The ammonite family Hildoceratidae in the Lower Jurassic of Britain. Monograph of the Palaeontolographical Society 586: 1–106; [pls. 1–16] 590: 107–200. [pls. 17–38] https://doi.org/10.1080/25761900.2022.12131769

Jacquin T, Dardeau C, Durlet C, de Graciansky PC, Hantzpergue P (1998) An overview of 2nd-order transgressive/regressive facies cycles in Western Europe. In: de Graciansky PC, Hardenbol J, Jacquin T, Vail P (Eds) Mesozoic and Cenozoic Sequence Stratigraphy of European Basin. SEPM Special Publication 60: 445–467. https://doi.org/10.2110/pec.98.02.0445

Jenkyns HC (1988) The early Toarcian (Jurassic) anoxic event; stratigraphic, sedimentary and geochemical evidence. American Journal of Science 288: 101–151. https://doi.org/10.2475/ajs.288.2.101

Jordan H (1960) Paläontologische und stratigraphische Untersuchungen im Lias delta (Domerium) Nordwestdeutschlands. PhD Thesis, Eberhard-Karls-Universität, Tübingen, Germany, 178 pp. [9 pls]

Jordan H (1989) Geologische Wanderkarte Leinebergland 1:100000. Niedersächsisches Landesamt für Bodenforschung, Hannover. [1 map with short explanatory notes on backside]

Jordan H, Büchner KH, Gehrt E, Leiber C, Lepper J, Scherler PC, Simon P, Stein V (1994) Geologische Karte von Niedersachsen. Erläuterungen zu Blatt Nr. 4024 Alfeld. Hannover (NLfB), 126 pp. [+1 map]

Jordan R, Schmidt-Kaler H (1985) Der Obere Lias (Toarcium) in Südfranken aufgrund neuer Bohrungen. Geologisches Jahrbuch, A 84: 55–101.

Kaiser M (2021) Untersuchungen zur Klärung paläogeographischer Fragen im Pliensbachium/Toarcium-Grenzbereich des Weser- und Osnabrücker Berglandes, unter besonderer Berücksichtigung des Massenaussterbens. PhD Thesis, Johann Wolfgang Goethe-Universität, Frankfurt am Main, Germany, 295 pp. [38 pls]

Keupp H, Arp G (1990) Aphotische Stromatolithe aus dem süddeutschen Jura (Lias, Dogger). Berliner Geowissenschaftliche Abhandlungen A124: 3–33.

Knitter H, Ohmert W (1983) Das Toarcium an der Schwärze bei Badenweiler (Oberrheingebiet S Freiburg). Jahreshefte des Geologischen Landesamtes Baden-Württemberg 25: 233–281.

Knoth W, Martiklos G, Lippstreu L (2000) Geologische Übersichtskarte 1 : 200000, Blatt CC 3934 Magdeburg. BGR, Hannover. [1 map]

Koert W (1923) Ein neuer Aufschluß in den Grenzschichten von Dogger und Lias im oberen Allertal. Jahrbuch der Preußischen Geologischen Landesanstalt zu Berlin 42 (1921): 525–532.

Kolb H (1942) Die Belemniten des jüngeren Lias z in Nordbayern. Zeitschrift der Deutschen Geologischen Gesellschaft 94: 145–168.

Krause T, Katzung G (1999) Die Kleintektonik im Lias am NE-Abhang des Röhnberges bei Wandersleben (Hainich-Saalfelder Störungszone). Veröffentlichungen des Naturkundemuseums Erfurt 18: 21–48.

Kriebel U, Martiklos G, Standke G (1998) Geologische Übersichtskarte 1 : 200000, Blatt CC 4734 Leipzig. BGR, Hannover. [1 map]

Kumm A, Riedel L, Schott W (1941) Das Mesozoikum in Niedersachsen. 1. Abteilung: Trias und Lias. Geologie und Lagerstätten Niedersachsens 2 (1), Stalling, Oldenburg, 328 pp.

Lacroix P, Le Pichon JP (2011) Les Hildoceratidae du Lias Moyen et Superieur des Domaines NW Européen et Tethysien. Une histoire de Famille. Dedale Editions, Lyon, 659 pp. [152 pls]

Lehmann U (1966) Dimorphismus bei Ammoniten der Ahrensburger Lias-Geschiebe. Paläontologische Zeitschrift 40: 26–55. https://doi.org/10.1007/BF02987629

Littke R, Rullkötter J (1987) Mikroskopische und makroskopische Unterschiede zwischen Profilen unreifen und reifen Posidonienschiefers aus der Hilsmulde. Facies 17: 171–180. https://doi.org/10.1007/BF02536781

Loh H, Maul B, Prauss M, Riegel W (1986) Primary production, maceral formation and carbonate species in the Posidonia shale of NW Germany. In: Degens ET, Meyers PA, Brassel SC (Eds) Biogeochemistry of black shales. Mitteilungen aus dem Geologisch-Paläontologischen Institut der Universität Hamburg 60: 397–421.

Look ER, Jordan H, Kolbe H, Meyer KD (1986) Geologische Wanderkarte 1:100000 Braunschweiger Land. Nördliches Harzvorland, Asse, Elm-Lappwald, Peine-Salzgitter, Allertal. 2nd extended edition, Niedersächsisches Landesamt für Bodenforschung, Hannover. [1 map]

Look ER, Kolbe H, Goldberg G, Jordan H, Kosmahl W, Meyer HJ, Meyer KD (1984) Geologie, Bergbau und Urgeschichte im Braunschweiger Land. Nördliches Harzvorland, Asse, Elm-Lappwald, Peine-Salzgitter, Allertal. Geologisches Jahrbuch A78: 1–452. [+1 map]

Ludwig G, Jordan R, Gramann F (1976) Schichtenverzeichnis „Hildesheim 5". Unpublished drilling report [3825SE0246], Niedersächsisches Landesamt für Bodenforschung, Hannover, 2 pp.

Lutikov OA, Arp G (2022) Taxonomy and biostratigraphic significance of the Toarcian bivalves of the genus *Meleagrinella* Whitfield, 1885. Stratigraphy and Geological Correlation 30(Suppl. 1): S47–S77. https://doi.org/10.1134/S0869593823010045

Lutz M, Etzold A, Käding KC, Lepper J, Hagdorn H, Nitsch E, Menning M (2006) Lithofazies und Leitflächen: Grundlagen einer dualen lithostratigraphischen Gliederung. Newsletters on Stratigraphy 41: 211–223. https://doi.org/10.1127/0078-0421/2005/0041-0211

NACSN [North American Commission on Stratigraphic Nomenclature] (1983) North American Stratigraphic Code. American Association of Petroleum Geologists Bulletin 67: 841–875.

NACSN [North American Commission on Stratigraphic Nomenclature] (2021) North American stratigraphic code. Stratigraphy 18: 153–204.

Maisch MW (2021) Neubewertung der Ammonitenfauna der Posidonienschiefer-Formation (Unterjura, Toarcium) von Baden-Württemberg, Südwestdeutschland. Jahreshefte der Gesellschaft für Naturkunde in Württemberg 177: 265–347. https://doi.org/10.26251/jhgfn.177.2021.265-347

Martiklos G (2002) Geologische Übersichtskarte von Sachsen-Anhalt im Maßstab 1:400000. Karte ohne quartäre Bildungen. Landesamt für Geologie und Bergwesen Sachsen-Anhalt, Halle/Saale. [1 map]

Martini HJ (1953) Salzsättel und Deckgebirge. Zeitschrift der Deutschen Geologischen Gesellschaft 105: 823–836. https://doi.org/10.1127/zdgg/105/1955/823

Maul B (1984) Untersuchungen zur Sedimentologie und Fazies an einem Profil im Oberen Lias bei Hildesheim, GK 25 Blatt Hildesheim, Nr. 3825. Diploma Thesis part 2, Georg-August-Universität, Göttingen, Germany.

Merkel A, Munnecke A (2023) Glendonite-bearing concretions from the upper Pliensbachian (Lower Jurassic) of South Germany: indicators for a massive cooling in the European epicontinental sea. Facies 69: 10. https://doi.org/10.1007/s10347-023-00667-6

Motzka R, Horn M, Hinze C, Jordan H, Lepper J, Reuter G, Waldeck H, Dahm HD (1979) Geologische Übersichtskarte 1:200000, Blatt CC 4718 Kassel. BGR, Hannover. [1 map]

Motzka-Nöring R (1998) Geologische Übersichtskarte 1:200000, Blatt CC 5518 Fulda. BGR, Hannover. [1 map]

Ohmert W, Wonik T, Rolf C, Martin M, Höhndorf A, Wetzel A, Allia V, Riegraf W, Baldanza A, Mattioli E, Bucefalo Palliani R, de Kaenel E, Bergen JA, Goy A, Ureta S, Arias C, Canales ML, Garcia Joral F, Herrero C, Martinez G, Perilli N (1996) Die Grenzziehung Unter–, Mitteljura (Toarcium, Aalenium) bei Wittnau und Fuentelsaz. Beispiele interdisziplinärer geowissenschaftlicher Zusammenarbeit. Informationen Geologisches Landesamt Baden–Württemberg 8: 52 pp.

Ott S (1967) Beitrag zur Kenntnis der stratigraphischen, paläogeographischen und tektonischen Verhältnisse der östlichen Subherzynen Kreidemulde. PhD Thesis, University of Greifswald, Germany, 130 pp.

Palfy J, Smith PL (2000) Synchrony between Early Jurassic extinction, oceanic anoxic event, and the Karoo-Ferrar flood basalt volcanism. Geology 28: 747–750. https://doi.org/10.1130/0091-7613(2000)28<3C747:SBEJEO>3E2.0.CO;2

Paul J (1993) Anatomie und Entwicklung eines permotriassischen Hochgebietes: die Eichsfeld-Altmark-Schwelle. Geologisches Jahrbuch A131: 197–218.

Pienkowski G (2004) The epicontinental Lower Jurassic of Poland. Polish Geological Institute Special Papers 12: 2–122.

Pinard JD, Weis R, Neige P, Mariotti N, Di Cencio A (2014) Belemnites from the Upper Pliensbachian and the Toarcian (Lower Jurassic) of Tournadous (Causses, France). Neues Jahrbuch für Geologie und Paläontologie, Abhandlungen 273: 155–177. https://doi.org/10.1127/0077-7749/2014/0421

Pratt BR, Finney SC, Easton RM, Piller WE (2023) Lithostratigraphy: Formation of the Formation. Newsletters on Stratigraphy 56: 307–330. https://doi.org/10.1127/nos/2022/0732

Quenstedt FA (1845–1849) Cephalopoden. Petrefactenkunde Deutschlands, 1.Abt. 1845: 1–104 [pls. 1–6]; 1846: 105–184, [pls. 7–12]; 1847: 185–264, [pls. 13–18]; 1848: 265–472, [pls. 19–30]; 1849: 473–580. [pls. 31–36] [Tübingen (Fues)]

Radzinski KH, Kästner H, Seidel G, Wiefel H, Berger HJ (1999) Geologische Übersichtskarte 1:200000, Blatt CC 5534 Zwickau. BGR, Hannover. [1 map]

Reinhold K, Krull P, Kockel F, Lutz R, Gaedicke C (2008) Geologische Karte 1:500000 Salzstrukturen Norddeutschland. BGR, Hannover. [1 map]

Riegel W, Loh H, Maul B, Prauss M (1986) Effects and causes in a Black Shale event. The Toarcian Posidonia Shale of NW Germany. Lecture Notes in Earth Sciences 8: 267–276. https://doi.org/10.1007/BFb0010214

Riegraf W (1985) Mikrofauna, Biostratigraphie und Fazies im Unteren Toarcium Südwestdeutschlands und Vergleiche mit benachbarten Gebieten. Tübinger Mikropaläontologische Mitteilungen 3: 1–232.

Riegraf W (1996) Belemniten im Ober-Toarcium und Unter-Aalenium Südwestdeutschlands. In: Ohmert W (Ed.) Die Grenzziehung Unter–, Mitteljura (Toarcium, Aalenium) bei Wittnau und Fuentelsaz. Beispiele interdisziplinärer geowissenschaftlicher Zusammenarbeit. Informationen Geologisches Landesamt Baden–Württemberg 8: 26–29.

Riegraf W (2000) The belemnites described by Baron Ernst Friedrich von Schlotheim (1764–1832). Paläontologische Zeitschrift 74: 281–303. https://doi.org/10.1007/BF02988102

Riegraf W, Werner G, Lörcher F (1984) Der Posidonienschiefer – Biostratigraphie, Fauna und Fazies des südwestdeutschen Untertoarciums (Lias epsilon). Enke, Stuttgart, 195 pp.

Roemer FA (1836) Die Versteinerungen des Norddeutschen Oolithengebirges. Hahn'sche Hofbuchhandlung, Hannover, 218 pp. [16 pls] https://doi.org/10.5962/bhl.title.118663

Röhl HJ, Schmid-Röhl A, Oschmann W, Frimmel A, Schwark L (2001) The Posidonia Shale (Lower Toarcian) of SW-Germany: an oxygen-depleted ecosystem controlled by sea level and palaeoclimate. Palaeogeography, Palaeoclimatology, Palaeoecology 165: 27–52. https://doi.org/10.1016/S0031-0182(00)00152-8

Röhl HJ, Schmid-Röhl A (2005) Lower Toarcian (Upper Liassic) black shales of the Central European Epicontinental Basin: A sequence stratigraphic case study from the SW German Posidonia Shale. In: Harris NB (Ed.) The deposition of organic-carbon-rich sediments. Models, mechanisms, and consequences. SEPM Special Publication 82: 165–189. https://doi.org/10.2110/pec.05.82.0165

Ruebsam W, Schwark L (2021) Impact of a northern-hemispherical cryosphere on late Pliensbachian–early Toarcian climate and environment evolution. In: Reolid M, Duarte L V, Mattioli E, Ruebsam W (Eds) Carbon Cycle and Ecosystem Response to the Jenkyns Event in the Early Toarcian (Jurassic), Geological Society, London, Special Publications 514: 359–385. https://doi.org/10.1144/SP514-2021-11

Rulleau L (2007) Biostratigraphie et paléontologique du Lias supérieur et du Dogger de la région Lyonnaise. Tome 1. Dédale Editions, Lafarge Ciments, 129 pp.

Rulleau L, Lacroix P, Becaud M, Le Pichon JP (2013) Les Dactylioceratidae du Toarcien Inferieur et Moyen. Une famille cosmopolite. Dedale Editions, Lyon, 244 pp. [46 pls]

Schlegelmilch R (1998) Die Belemniten des süddeutschen Jura. Fischer, Stuttgart, 151 pp. [20 pls] https://doi.org/10.1007/978-3-8274-3083-0

Schmitz HH (1968) Untersuchungen am nordwestdeutschen Posidonienschiefer und seiner organischen Substanz. Beihefte zum Geologischen Jahrbuch 58: 1–220.

Schroeder H (1912) Geologische Spezialkarte von Preussen und den Thüringischen Staaten und Nachfolgewerke, [Neue Nr. 3927] Ringelheim, Gradabteilung 41, Blatt 60. Kraatz, Berlin. [1 map] https://doi.org/10.23689/fidgeo-3550

Schulbert C (2001) Die Ammonitenfauna und Stratigraphie der Tongrube Mistelgau bei Bayreuth (Oberfranken). Beihefte zu den Berichten der Naturwissenschaftlichen Gesellschaft Bayreuth 4: 1–183.

Seidel G, Kästner H, Wiefel H (1998) Geologische Übersichtskarte 1 : 200000, Blatt CC 5526 Erfurt. BGR, Hannover. [1 map]

Thomas E (1924) Genetische Betrachtungen über die Lias- und Neokomablagerungen am Fallstein und ihre Eisenerze. Jahrbuch des Halleschen Verbandes für die Erforschung der mitteldeutschen Bodenschätze und ihrer Verwertung 4: 74–155.

van de Schootbrugge B, Richoz S, Pross J, Luppold FW, Hunze S, Wonik T, Blau J, Meister C, van de Meijst CMH, Suan G, Fraguas A, Fiebig J, Herrle JO, Guex J, Little CTS, Wignall PB, Püttmann W, Oschmann W (2019) The Schandelah Scientific Drilling Project: A 25-million year record of Early Jurassic palaeoenvironmental change from northern Germany. Newsletters on Stratigraphy 52: 249–296. https://doi.org/10.1127/nos/2018/0259

Vinken R (1971) Geologische Karte von Niedersachsen 1:25 000. Erläuterungen zu Blatt Dingelbe Nr. 3826. Ergänzungsheft. Niedersächsisches Landesamt für Bodenforschung, Hannover, 189 pp.

Visetin S, Erba E, Mutterlose J (2022) Bio- and chemostratigraphy of the Posidonia Shale: a new database for the Toarcian Oceanic Anoxic Event from northern Germany. Newsletters on Stratigraphy 55: 173–198. https://doi.org/10.1127/nos/2021/0658

Voigt T, von Eynatten H, Franzke HJ (2004) Late Cretaceous unconformities in the Subhercynian Cretaceous Basin (Germany). Acta Geologica Polonica 54(4): 673–694.

von Eynatten H, Voigt T, Meier A, Franzke HJ, Gaupp R (2008) Provenance of Cretaceous clastics in the Subhercynian Basin: constraints to exhumation of the Harz Mountains and timing of inversion tectonics in Central Europe. International Journal of Earth Sciences (Geologische Rundschau) 97: 1315–1330. https://doi.org/10.1007/s00531-007-0212-0

von Seebach K (1864) Der Hannoversche Jura. Verlag von Wilhelm Hertz, Berlin, 158 pp. [9 pls]

Waldeck H (1986) Geologische Übersichtskarte 1 : 200000, Blatt CC 4726 Goslar. BGR, Hannover. [1 map]

Weis R (1999) Die Belemniten der Minette-Formation (ob. Toarcium - ob. Aalenium) Luxemburgs. In: Delsate D, Duffin C, Weis R (Eds) Les collections paléontologiques du Musée national d'histoire naturelle de Luxembourg. Fossiles du Trias et du Jurassique. Travaux scientifiques du Musée national d'histoire naturelle de Luxembourg 32: 201–246.

Weitschat W (1973) Stratigraphie und Ammoniten des höheren Untertoarcium (oberer Lias e) von NW-Deutschland. Geologisches Jahrbuch A8: 3–31.

Wunnenberg C (1928) Beiträge zur Kenntnis des Lias epsilon in der Umgebung Braunschweigs. Jahresbericht des Vereins für Naturwissenschaft Braunschweig 20: 56–80.

Wunnenberg C (1950) Zur Ausbildung des Posidonienschiefers in der Umgebung von Braunschweig, mit besonderer Berücksichtigung der Fossilisation. Neues Jahrbuch für Geologie und Paläontologie, Monatshefte 1950(5–6): 146–182.

Xu W, Ruhl M, Jenkyns HC, Leng MJ, Huggett JM, Minisini D, Ullmann CV, Riding JB, Weijers JWH, Storm MS, Percival LME, Tosca NJ, Idiz EF, Tegelaar EW, Hesselbo SP (2018) Evolution of the Toarcian (Early Jurassic) carbon-cycle and global climatic controls on local sedimentary processes (Cardigan Bay Basin, UK). Earth and Planetary Science Letters 484: 396–411. https://doi.org/10.1016/j.epsl.2017.12.037

Ziegler PA (1990) Geological atlas of western and central Europe. 2nd edn., Shell Internationale Petroleum Maatschapij B.V., Den Haag, 56 enclosures.

Zimmermann J, Franz M, Heunisch C, Luppold FW, Mönnig E, Wolfgramm M (2015) Sequence stratigraphic framework of the Lower and Middle Jurassic in the North German Basin: Epicontinental sequences controlled by Boreal cycles. Palaeogeography, Palaeoclimatology, Palaeoecology 440: 395–416. https://doi.org/10.1016/j.palaeo.2015.08.045

Supplementary material 1

Measurements of belemnite alignments in the Posidonienschiefer and Jurensismergel Formations, Toarcian, Hainberg section

Authors: Gernot Arp, Yagmur Balmuk, Stephan Seppelt, Andreas Reimer

Data type: xls

Link: https://doi.org/10.3897/zitteliana.97.110677.suppl1

Supplementary material 2

Selected biofacies of the Toarcian to lowermost Aalenian succession, Hainberg section

Authors: Gernot Arp, Yagmur Balmuk, Stephan Seppelt, Andreas Reimer
Data type: jpg
Explanation note: (1) *Parainoceramya* biofacies, bed 11 "Boreale Concretions", middle Posidonienschiefer Formation. GZG.INV.891. (2) *Bositra buchi* biofacies, bed 21, middle Posidonienschiefer Formation. GZG.INV.892. (3) Cephalopod-free dwarf *Bositra buchi* biofacies, 9 m above basis of bed 24, upper Posidonienschiefer Formation. GZG.INV.893. (4) *Chlamys textoria* biofacies, bed 27 "oolite marl", Jurensismergel Formation. GZG.INV.894. (5) Nubeculariid foraminifera on bioclasts of the *Chlamys textoria* biofacies. Bed 29, Jurensismergel Formation. GZG.INV.895. (6) *Bositra suessi* biofacies, 80 cm above basis of bed 40, Opalinuston Formation. GZG.INV.896.

Link: https://doi.org/10.3897/zitteliana.97.110677.suppl2

Supplementary material 3

Columnar section from the middle part of the Posidonienschiefer Formation at Listringen

Authors: Gernot Arp, Yagmur Balmuk, Stephan Seppelt, Andreas Reimer
Data type: jpg
Explanation note: According to Vinken (1971).

Link: https://doi.org/10.3897/zitteliana.97.110677.suppl3

Supplementary material 4

Columar section of the lower and middle Posidonienschiefer Formation at Hildesheim-Itzum

Authors: Gernot Arp, Yagmur Balmuk, Stephan Seppelt, Andreas Reimer
Data type: jpg
Explanation note: According to Maul (1984), Loh et al. (1986), and Riegel et al. (1986).

Link: https://doi.org/10.3897/zitteliana.97.110677.suppl4